ON THE DYNAMICS OF JOSEPHSON JUNCTION CIRCUITS

by

A.A. Abidi and L.O. Chua

Memorandum No. UCB/ERL M78/42

5 July 1978

ELECTRONICS RESEARCH LABORATORY

College of Engineering
University of California, Berkeley
94720

ON THE DYNAMICS OF JOSEPHSON JUNCTION CIRCUITS†

A. A. Abidi and L. O. Chua††

ABSTRACT

A qualitative theory of the circuit dynamics of the Josephson junction device using a simple circuit model is developed. By examining trajectories on a cylindrical phase space and on the surface of a torus, respectively, the main features of the I-V characteristics of the junction excited by d.c. and a.c. are explained, and their properties derived. These results lead to the interpretation of the steps of constant voltage in the a.c. characteristics as a manifestation of the synchronization phenomenon.

† Research supported in part by the Office of Naval Research Contract N00014-76-C-0572 and the National Science Foundation Grant ENG77-22745.

†† A. A. Abidi and L. O. Chua are with the Department of Electrical Engineering and Computer Science and the Electronics Research Laboratory, University of California, Berkeley, California 94720

1. Introduction

The Nobel Prize in Physics was awarded to B. Josephson in 1973 for his discovery of the quantum-mechanical tunnelling of carriers through an insulator sandwiched between two superconducting metals. The phenomenon has been termed the Josephson effect since its discovery in 1962 [1], and electrical devices which use this effect for conduction are called Josephson junction devices. Although seemingly esoteric, the electromagnetic properties of Josephson junctions have been used in applications ranging from the measurement of minute magnetic fields [2] to the fastest known digital computers with picosecond switching times [3].

Scientific articles related to this effect have constantly appeared in solid state journals, both in the Western world and the U.S.S.R., since the announcement of this effect. With a few interesting exceptions [4], these articles are either quantum-mechanical analyses of the effect or sundry reports of experiments which reveal some very remarkable phenomena associated with circuits containing Josephson junctions. Those who have ventured to solve the differential equations of Josephson junction circuits have necessarily restricted themselves to approximate methods [5-6], or to the use of approximate analogue models [7]. The situation remains somewhat unsatisfactory from the circuit theorist's point of view as only a very limited insight is available into the general circuit behavior of the device.

Our research has concerned itself with developing a unified qualitative theory of the phenomena associated with Josephson junction circuits. To this end, we have used some results from the theory of differential equations which provide greater insight into the highly nonlinear behavior of this remarkable two-terminal device. At the outset we acknowledge the 1970 paper by Waldram, Pippard and Clark [4] which has provided us consistently with insights during our research.

2. Modeling the Device

We chose to use the simplest available device model in our investigations, for to use a detailed model would obscure the essential phenomena which the device portrays in simple circuits. Our device model (Fig. 1) is the simple one proposed by McCumber [8]. The nonlinear tunnelling phenomenon produces

a current $I_o \sin \phi$, where ϕ is the phase difference of the quantum mechanical wave function across the junction. Furthermore, one of Josephson's central results proved that the junction voltage is given by

$$v(t) = \frac{\bar{h}}{2e} \frac{d\phi}{dt} , \quad \bar{h} = h/2\pi ,$$

where h and e denote Planck's constant and electron charge, respectively. In circuit theoretic terms, the tunnelling current can thus be modeled by a non-linear flux-controlled inductor. There is another current, attributed to quasiparticle effects, which is modeled as the linear resistor R. The physical capacitance of the dielectrically separated superconductors is represented by C. Typical values are $I_o = 10^{-5}$ A, $R = 10^{-7}\Omega$ and C = 10nF.

Summing currents in Fig. 1, we obtain

$$\begin{aligned} i &= I_o \sin \phi + \frac{v}{R} + C \frac{dv}{dt} \\ &= I_o \sin \phi + \frac{h}{2eR} \frac{d\phi}{dt} + \frac{\bar{h}C}{2e} \frac{d^2\phi}{dt^2} \end{aligned} \tag{1}$$

Other models for the Josephson junction often non-electrical in nature exist in the literature. Notable amongst these is the rotating disc model [9], the motion of a pendulum in viscous fluid [4], and the phase locked loop [10]. The differential equations describing these models resemble the preceding equation (1).

3. The d.c. Excited Josephson Junction

The simplest means of exciting a Josephson junction is to impress a direct current across its two terminals. Experiments show that a non-sinusoidal oscillation of the voltage results [11], whose fundamental frequency is of the order of gigahertz. At these frequencies, it is only reasonable to experimentally specify the junction characteristics by plotting the average (or d.c.) value of the voltage waveform as a function of the exciting direct current. Typical characteristics of a point-contact junction taken from [8] are given in Fig. 2.

It is of interest to note that these characteristics can vary markedly

for junctions of different physical constructions and geometries. The main features common to all these characteristics are as follows:

(i) A current can be maintained through the device with zero voltage across it. This is the supercurrent region of operation.

(ii) For large current excitations beyond the critical value I_o, the device abruptly attains a finite voltage.

(iii) A peculiar hysteresis is displayed in the characteristics, as follows. For an increasing excitation I, the transition from the supercurrent to finite voltage occurs abruptly at I_o, but if the excitation is now decreased, the transition from finite voltage to supercurrent occurs smoothly at some $I_c < I_o$.

Although (1) has not been solved analytically, [5] and [8] have verified both the supercurrent and the asymptotic regions of Fig. 2. Furthermore, McCumber has calculated the variation in the hysteresis threshold, I_c, as a function of the junction capacitance. His results are plotted in Fig. 3.

4. Circuit Dynamics in a Cylindrical Phase Space

Under direct current excitation $i = I_{dc}$, (1) becomes

$$\frac{\bar{h}C}{2e}\frac{d^2\phi}{dt^2} + \frac{\bar{h}}{2eR}\frac{d\phi}{dt} + I_o \sin\phi = I_{dc}$$

$$\text{i.e. } \frac{d^2\phi}{dt^2} + \frac{1}{RC}\frac{d\phi}{dt} + \left(\frac{2e}{\bar{h}C}\right) I_o \sin\phi = \left(\frac{2e}{\bar{h}C}\right) I_{dc} \qquad (2)$$

This equation can be expressed in a normalized form by defining the dimensionless variables

$$\alpha \triangleq \frac{I_{dc}}{I_o}, \quad \omega_o \triangleq \frac{2e}{\bar{h}} I_o R, \quad \tau \triangleq \omega_o t \qquad \beta_c \triangleq \omega_o RC$$

so that (2) becomes

$$\frac{d^2\phi}{d\tau^2} + \frac{1}{\beta_c}\frac{d\phi}{d\tau} + \frac{1}{\beta_c}\sin\phi = \frac{\alpha}{\beta_c} \qquad (DC)$$

Now if we define $x \triangleq \phi$, $y \triangleq \frac{dx}{d\tau} = \frac{d\phi}{dt}$, (DC) can be expressed in the state equation form as follows:

$$\left.\begin{aligned} \dot{x} &= f_1(x,y) \triangleq y \\ \dot{y} &= f_2(x,y) \triangleq \frac{1}{\beta_c}(\alpha - y - \sin x) \end{aligned}\right\} \tag{3}$$

These are autonomous, or time-invariant state equations, insofar as the time variable does not appear explicitly on the right-hand side. In fact, time can be eliminated altogether from (3) by rewriting it as

$$\frac{dy}{dx} = F(x,y) \triangleq \frac{f_2(x,y)}{f_1(x,y)} = \frac{\alpha - y - \sin x}{\beta_c y} \tag{4}$$

Geometrically, solutions of (3) define trajectories in the three-dimensional space $\sum x\ t$, where

$\sum$ = Two-dimensional state space (or the phase plane)

t = Independent time variable

Typical trajectories in $\sum x\ t$ and their projections in the phase plane $\sum$ are shown in Figs. 4(a) and 4(b), respectively.

Notice, however, that (4) has the very special periodic property that

$$\frac{dy}{dx} = f(x,y) = f(x+2\pi, y)$$

which means that the direction field[1] defined by (4) in $\sum$ is 2π-periodic with respect to the state variable x. Thus, the direction field can be uniquely defined, modulo 2π in x, by restricting $\sum$ to the strip $[0,2\pi) \times \mathbb{R}$. To visualize continuous flows[2] produced by this direction field, this strip can be smoothly transformed into a cylinder ($\sum'$) by joining its two ends (Fig. 5). A typical flow on the surface of the cylinder $\sum'$ is also illustrated.

The state equations (3) possess an equilibrium point at $(\hat{x},\hat{y})$ if $f_1(\hat{x},\hat{y}) = 0$ and $f_2(\hat{x},\hat{y}) = 0$. Clearly this occurs at the points $\hat{y} = 0$, $\hat{x} = \arcsin \alpha$ and $(\pi - \arcsin \alpha)$, i.e., $(\arcsin \alpha, 0)$ and $(\pi - \arcsin \alpha, 0)$ are the two equilibrium points in $\sum$. For $\alpha < 1$, these points lie symmetrically on either side of the point $\left(\frac{\pi}{2},0\right)$. For $\alpha = 1$, the points come together and coalesce at $\left(\frac{\pi}{2},0\right)$, and for $\alpha > 1$, they disappear altogether.

The nature of these equilibrium points can be one of three types: node,

---

[1] Henceforth, a vector field defined on a state space $\sum$ is called a direction field.

[2] The integral curves in a state space $\sum$ resulting from a given direction field are called flows.

focus or saddle point [12]. The type of equilibrium point and its stability is determined by examining the signs of T, Δ and $T^2 - 4\Delta$ [12] where

$$T \triangleq \frac{2f_1}{2x} + \frac{2f_2}{2y} \text{ and } \Delta \triangleq \det \begin{bmatrix} \frac{2f_1}{2x} & \frac{2f_1}{2y} \\ \frac{2f_2}{2x} & \frac{2f_2}{2y} \end{bmatrix}$$

So for (3), $T = -\frac{1}{\beta_c}$, $\Delta = \frac{1}{\beta_c} \cos \hat{x}$.

Thus, the equilibrium point (arc sin α, 0) is a <u>stable node</u> if $\beta_c < \frac{1}{4 \text{ arc sin } \alpha}$.

or a <u>stable focus</u> if $\beta_c > \frac{1}{4 \text{ arc sin } \alpha}$, whereas the equilibrium point

(π - arcsin α, 0) will always be a <u>saddle</u> point.

Differential equations of the form $\frac{dy}{dx} = F(x,y) = F(x+2\pi, y)$ yield flows on the cylinder $\sum'$ with some very interesting properties, which have been detailed in the treatise of Pliss [17]. We state these properties below and provide detailed proofs for some of them in Appendix 1. The reader is referred to [17] for a complete exposition.

We define a flow $y = \phi(x)$ in $\sum = \mathbb{R}^2$ to be <u>2π x - periodic</u> if $\phi(x+2\pi) = \phi(x)$, $\forall\, x \in \mathbb{R}$. On the cylinder $\sum'$, a 2π x - periodic flow will describe a closed loop.

<u>Theorem 1.</u> If a unique solution $y = \phi(x)$ of (4) through (x_o, y_o) exists for all $x > x_o$ in $\sum$, and is bounded then it is either 2π x-periodic or asymptotically approaches some 2π x - periodic solution as $x \to \infty$.

Thus, if the solution does not approach an equilibrium point as $x \to \infty$, then it must tend to a 2π x-periodic solution. Perceptive readers will recognize the similarity between this result and the Poincare-Bendixson theorem [13].

<u>Theorem 2.</u> Any unique solution $y = \phi(x)$ of (4) is bounded either above or below as $x \to \infty$.

We have plotted accurate phase plane portraits for the solutions of (4) in Appendix 2, for a range of typical values of α and β_c. These portraits suggest the following general properties for these solutions of (4):

(i) For α greater than a critical value, an equilibrium point and a 2π x-periodic solution coexist.

(ii) The trajectories which converge asymptotically to either an equilibrium point or a 2π x-periodic solution are separated by the separatrix trajectory, which is the trajectory passing through the saddle point (π - arc sin α, 0). Thus, if $y_s(0)$ is the initial condition of the separatrix on $\sum'$, then all trajectories with initial condition $y(0) > y_s(0)$ tend to a 2π x-periodic solution, and all trajectories with $y(0) < y_s(0)$ tend to the equilibrium point (sin α, 0).

(iii) Keeping α constant, the 2π x-periodic solution may be made to disappear altogether if β_c is made large enough.

Using these phase plane portraits, we have devised a simple and efficient numerical procedure based on the shooting method [18] to calculate the hysteresis in the I-V characteristics. Our procedure and results are given in Appendix 2.

It is instructive to visualize the flows on the surface of $\sum'$ as trajectories[3] in $\sum' \times \tau$. As $\sum'$ is the surface of a cylinder, $\sum' \times \tau$ can be thought of as a series of equally spaced concentric cylinders, where each cylinder is an isochrone; i.e., the radius of any cylinder specifies the time variable (Fig. 6). Suppose now that there exists a 2π x-periodic flow on $\sum'$, which will define the loop $\mathcal{L}(\alpha,\beta_c) \triangleq \{(x,y) | y(x+2\pi) = y(x), x \in [0,2\pi)\}$ on $\sum'$. Then the surface defined by $\mathcal{L}(\alpha,\beta_c) \times \tau$ will be an integral manifold [14] for this periodic solution; that is, if (x_o,y_o,τ_o) is a point in this surface, then $\left(x(\tau),y(\tau),\tau\right)$ lies on this surface for $\tau > \tau_o$, where $\left(x(\tau),y(\tau),\tau\right)$ is the trajectory described by the solutions of (4) with initial conditions (x_o,y_o,τ). Because of the time-invariance of (4), the following properties are true:

Observation 1: $y = \phi(x)$ is 2π x-periodic on $\sum'$ if, and only if, the trajectory $\left(x(\tau),\phi(x(\tau)),\tau\right)$ is time periodic in $\sum' \times \tau$,

i.e., $\exists\ T > o \ni x(\tau+T) = x(\tau) + 2\pi,\ y(\tau+T) = y(\tau),\ \forall\tau$

Thus, Theorem 1 has proved that if the state variables x and y do not attain an equilibrium point, then they produce time periodic waveforms as $\tau \to \infty$. We can also see how the time period of these waveforms varies as a function of α.

---

[3] Integral curves in space-time $\sum \times \tau$ are called trajectories.

Observation 2: Let (4) possess a periodic solution for $\alpha = \hat{\alpha}$ with time period $\hat{T}$. For any $\varepsilon > o$ $\exists\, \delta > o$ such that if $\alpha = \hat{\alpha} + \varepsilon$ in (4), it will still possess a periodic solution, and the time period of this oscillation will be $(\hat{T}-\delta)$.

Proof: The proof relies on two facts observed from the phase plane portraits of Appendix 2:

(a) If, for a fixed β_c, $\alpha = \hat{\alpha}$ yields a 2π x-periodic solution, then all $\alpha > \hat{\alpha}$ will also yield a 2π x-periodic solution.

(b) For any $\varepsilon > o$ the periodic solution trajectory in the x-y plane corresponding to $(\alpha+\varepsilon)$ lies above the trajectory corresponding to α. More precisely, $y_{\alpha+\varepsilon}(x) > y_{\alpha}(x)$, $\forall\, x \in [0,2\pi)$. In the $\sum'$ x τ space of Fig. 6, this means that the integral manifold for the periodic solution due to α lies above the integral manifold for the periodic solution due to α.

Fact (a) thus establishes the existence of periodic solutions above a threshold value of α. Fact (b) states that $\dot{\phi}_{\alpha+\delta}(\phi) > \dot{\phi}_{\alpha}(\phi)$ on the periodic solutions, $\forall\, \phi \in [0,2\pi)$.

$$\text{Now } \dot{\phi} = \frac{d\phi}{dt} \quad \Rightarrow \int_o^T dt = \int_o^{2\pi} \frac{d\phi}{\dot{\phi}(\phi)} \quad \Rightarrow T = \int_o^{2\pi} \frac{1}{\dot{\phi}(\phi)}\, d\phi$$

where T is the time period of the 2π x-periodic trajectory. Clearly, then $T_{\alpha+\varepsilon} < T_{\alpha}$ for $\varepsilon > o$, i.e., $\exists\, \delta > o$ s.t. $T_{\alpha+\varepsilon} = T_{\alpha} - \delta$. ∎

Observation 2 allows us to think of the Josephson junction as a current-controlled oscillator whose frequency of oscillation increases with increasing d.c. excitation applied at its terminals. This is an important interpretation to bear in mind when we later consider the behavior of the a.c. excited junction.

5. The a.c. Excited Josephson Junction

In connection with the application of Josephson junction devices as microwave generators and mixers [15], experimenters have looked at the characteristics of the device when, in addition to a d.c. bias, an alternating current of arbitrary angular frequency (ω) is applied at the terminals Fig. (7(a)). If the direct current excitation (the bias) is varied while keeping the alternating

current excitation constant, a set of direct current vs. average junction voltage characteristics is obtained. Some typical experimentally obtained characteristics are shown in Fig. 7 (b): the major effect of the a.c. excitation is to introduce regularly spaced constant voltage steps onto I-V characteristics which otherwise are similar to Fig. 2. In particular, the characteristics of Fig. 7(b) have the following features:

(i) The <u>average</u> voltage (V) is a monotonically increasing function of the d.c. excitation (I_{dc}): no negative resistance regions are observed.

(ii) The constant voltage steps appear at multiple and submultiple values of a fundamental voltage. The heights of these steps do not appear to follow a monotonic law.

(iii) The height of a given step is observed to vary with the amplitude of the a.c. excitation, I_{ac}. Some authors [4] suspect that this height varies as a suitable chosen Bessel function of I_{ac}.

(iv) The effect of varying the frequency, ω, of the a.c. excitation is to change the spacing between these steps.

Using the model of (1) with an a.c. excitation, we obtain a differential equation of the form

$$\frac{\bar{h}C}{2e}\frac{d^2\phi}{dt^2} + \frac{\bar{h}}{2eR}\frac{d\phi}{dt} + I_o \sin\phi = I_{dc} + I_{ac}\sin\omega t \qquad (5)$$

Again, the solutions of (5) will give trajectories in a cylindrical phase space, except now subject to a time-varying direction field.

To simplify the discussion, and more importantly, to avail ourselves of existing mathematical results, we neglect the second derivative term in (5) by letting C = 0. Although this is not physically justified, we believe that the second-order term does not signif. ntly alter the qualitative behaviors which follow. Roughly speaking, we needed the second-order term in the d.c. analysis to discover in detail the autonomous behavior of the circuit dynamics; in the a.c. case, the dynamics are governed largely by the a.c. or synchronizing excitation, and the first derivative is enough to reveal the basic behavior of (5).

The simplified differential equation then is:

$$\frac{\bar{h}}{2eR}\frac{d\phi}{dt} + I_o \sin\phi = I_{dc} + I_{ac}\sin\omega t \qquad (AC)$$

Consistent with the notation of the d.c. analysis, (AC) can be normalized by introducing the following dimensionless variables:

$$\Omega \triangleq \frac{\omega}{\omega_o} \quad , \quad \tilde{\alpha} \triangleq \frac{I_{ac}}{I_o} \quad ,$$

$$T \triangleq \Omega \tau \ ,$$

$$A_o \triangleq \frac{1}{\Omega} \quad , \quad A_{dc} \triangleq \frac{\alpha}{\Omega} \quad , \quad A_{ac} \triangleq \frac{\tilde{\alpha}}{\Omega}$$

whence (AC) becomes

$$\frac{d\phi}{dT} + A_o \sin \phi = A_{dc} + A_{ac} \sin T$$

or

$$\frac{d\phi}{dT} = A_{dc} - A_o \sin \phi + A_{ac} \sin T \tag{6}$$

We observe that the right-hand side of (6) is 2π periodic in both ϕ and T; this property is now exploited.

6. Circuit Dynamics on the Surface of a Torus

The differential equation (6) describes a single state variable ϕ. Thus, $\sum$ x T is a two-dimensional trajectory space. However, because the velocity field[4] defined by (6) on $\sum$ x T is 2π-periodic along both $\sum$ and T, diffeomorphic operations can be introduced to transform the Euclidean coordinates to the surface of a torus where ϕ and T are defined modulo 2π (Fig. 8). Consequently, a trajectory which lies in the plane $\sum$ x T will, after transformation, lie on the surface of the torus $\sum'$ x T'. A motion of 2π along a latitude on the torus is called a rotation and along a longitude is called a revolution (see Fig. 8).

The theory of flows on a torus, initially formulated by Poincare in connection with celestial mechanics [16], has been brought up to date by Pliss [17], and applies to any differential equation of the form $\frac{dy}{dx} = f(x,y)$ where $f(x+2\pi,y) = f(x,y+2\pi) = f(x,y)$. We interpret and develop these results in the following sections to understand the qualitative behavior of the solutions of (6).

---

[4] A vector field in space time $\sum$ x t is referred to as a velocity field.

7. Periodic Solutions on the Surface of a Torus

What does a periodic trajectory look like on the surface of a torus? Periodicity means that for some $T > 0$, $\phi(T+T) = \phi(T) \pmod{2\pi}$ for all T. On the torus surface, this corresponds to a trajectory which closes upon itself: three examples of such trajectories are shown in Fig. 9. These examples are fundamental insofar as <u>any</u> periodic trajectory can be classified as one of these three types. Fig. 9(a) illustrates the simplest case, where the trajectory executes one rotation and one revolution before closing upon itself. Fig. 9(b) is another possibility, where one revolution and six rotations are completed before closure, and Fig. 9(c) portrays one rotation and three revolutions being executed before closure. In the most general instance, q revolutions and p rotations will be completed before the trajectory closes upon itself.

The three examples of periodic motion in Fig. 9 have important physical interpretations. Fig. 9(a) represents an oscillatory waveform whose period along the normalized T coordinate is 2π, i.e., $2\pi/\omega$ sec. in <u>actual</u> time (t). Fig. 9(c) requires a period of $3 \times 2\pi = 6\pi$ in T, i.e., $6\pi/\omega$ sec. in t. The waveform in Fig. 9(b) advances ϕ by 2π radius in $\frac{1}{6} \times 2\pi = \pi/3$ in T due to the sinusoidal symmetry of the vector field generated by equation (6), i.e., a time period of $\pi/3\omega$ sec. Recall now that the period of the sinusoidal a.c. excitation applied to the junction is $2\pi/\omega$ sec. The oscillation of Fig. 9(a) has a period <u>identical</u> to that of the excitation, while that of Fig. 9(b) has a period which is the <u>6th harmonic</u> of the excitation, and that of Fig. 9(c) has a period which is the <u>3rd subharmonic</u> of the excitation.

In general if a trajectory executes p rotations and q revolutions before closing on itself, its frequency is equal to the <u>pth harmonic of the qth subharmonic</u> of the excitation frequency.

8. Conditions for the Existence of Periodic Solutions

We return to the two-dimensional Euclidean space $\Sigma \times T$ to obtain some properties of the periodic trajectories defined above. In accordance with Pliss, we consider $\Sigma \times T$ ($\equiv \mathbb{R}^2$) divided up into a grid of multiples of 2π Fig. 10(a) so that a periodic trajectory with initial condition $\phi(o) = 0$ must pass through some grid point $(2q\pi, 2p\pi)$: this corresponds to p rotations

and q revolutions executed on the surface of the torus $\sum' \times T'$ prior to closure.

Henceforth, $\phi = F(T,\phi_o)$ denotes the solution of (6) with initial condition $\phi(o) = \phi_o$. The following remarkable property holds for the trajectory of $F(T,0)$ plotted in the $\sum \times T$ plane:

Theorem 3: Let q and p be factorized as $q = Kq_1$ and $p = Kp_1$ (where K is an integer > 1), and assume that the grid point $(2q\pi,2p\pi)$ lies above (resp., below, on) the trajectory $F(T,0)$. Then the point $(2q_1\pi,2p_1\pi)$ will also lie above (resp., below, on) the trajectory.

Proof: See Appendix 3.

Thus, the ratio p/q contains sufficient information to uniquely specify whether the grid point $(2q\pi,2p\pi)$ lies above, below or on the trajectory $F(T,0)$. If we now assign the ratio corresponding to every grid point into one of the following two classes:

$$\text{Class 1} \triangleq \left\{ \frac{p}{q} \;\middle|\; F(T,0) \text{ passes } \underline{\text{below or through}} \text{ the grid point } (2q\pi,2p\pi) \right\} \text{ and}$$

$$\text{Class 2} \triangleq \left\{ \frac{p}{q} \;\middle|\; F(T,0) \text{ passes } \underline{\text{above}} \text{ the grid point } (2q\pi,2p\pi) \right\}$$

then these two classes have the following properties:

(i) Each class is non-empty.

(ii) Every rational number belongs either to Class 1 or to Class 2.

(iii) For every $x \in$ Class 1 and $y \in$ Class 2, $x > y$.

Class 1 and Class 2 thus define a Dedekind cut on the rational numbers Fig. 10(b). The real number (μ) delineated by this cut (which may be rational or irrational) is called the turning point, and is uniquely defined by given values of A_{dc}, A_{ac} and A_o in (6).

We can generalize this definition of turning point with the following important result:

Theorem 4: Let μ be the turning point generated by a given right-hand side of (6). Then if $F(T,\phi_o)$ is the trajectory in $\sum \times T$ generated by (6) for any $\phi_o \in [0,2\pi)$, the following limiting relation holds: $\lim_{T\to\infty} \frac{F(T,\phi_o)}{T} = \mu$

Proof: See Appendix 3.

Note that this result provides us with a purely algebraic interpretation of

the turning point for trajectories emanating from arbitrary initial conditions; the Dedekind cut interpretation derived from grid points is geometric, but only holds when the initial condition is 0. A very powerful result concerning the existence of periodic solutions can be obtained by considering the nature of the turning point.

Theorem 5: There exists a periodic solution trajectory of (6) on the torus $\sum' \times T'$ which completes p rotations and q revolutions prior to closing upon itself if, and only if, the turning point $\mu = \frac{p}{q}$.

Proof: See Appendix 3.

The interpretation of this result deserves a few remarks:

(i) A periodic solution with $\mu = p/q$ will satisfy $F(2q\pi,\phi_o) = \phi_o + 2p\pi$ for some $\phi_o \in [0,2\pi)$.

(ii) The junction voltage waveforms will be periodic whenever the average junction voltage V_{dc} is a rational multiple of $\hat{V}$.

(iii) If $\mu = p/q$, there may be more than one periodic solution on the torus $\sum' \times T'$, i.e., the cardinality of the set

$$\mathcal{N}(\mu) \triangleq \left\{ \phi_o \;\middle|\; F(2q\pi,\phi_o) = \phi_o + 2p\pi,\ \phi_o \in [0,2\pi) \right\}$$

may be greater than 1. However, all these periodic solutions must execute multiples of p_1 rotations and q_1 revolutions before closing upon themselves, where p_1 and q_1 are relatively prime integers and $\frac{p_1}{q_1} = \frac{p}{q}$.

Furthermore, we can show that these periodic solutions are stable.

Theorem 6: Assume that (6) has a rational turning point $\mu = p/q$. Then any non-periodic solution approaches a periodic solution as $T \to \infty$ and a possibly different periodic solution as $T \to -\infty$.

Proof: See [17]

Corollary: If we have an isolated periodic solution (i.e., $\bar{\phi}_o \in \mathcal{N}(\mu)$ and an $\varepsilon > 0$ such that $|\phi_o - \bar{\phi}_o| < \varepsilon \Rightarrow \phi_o \notin \mathcal{N}(\mu)$, and it is stable in the sense of Lyapunov [14, 17], then it is asymptotically stable.

Proof: See [17].

We now make some remarks on the number of periodic solutions that (6) will

possess if the turning point $\mu = \frac{p}{q}$. Let us define the determining function

$g(\phi_o) \triangleq F(2q\pi,\phi_o) - (\phi_o + 2p\pi)$: the zeros of this function on the interval $[0,2\pi)$ are then the elements of the set $\mathcal{N}(\mu)$. This function has the following properties:

(i) $g(\phi_o)$ is a continuous function of ϕ_o. This follows from the basic result in differential equation theory that the solution $F(2q\pi,\phi_o)$ is a continuous function of the initial condition ϕ_o. [14]

(ii) $g(\phi_o)$ is 2π periodic in ϕ_o. This is true because

$$g(\phi_o + 2\pi) = F(2q\pi,\phi_o + 2\pi) - (\phi_o + 2\pi + 2p\pi) =$$

$$F(2q\pi,\phi_o) + 2\pi - (\phi_o + 2\pi + 2p\pi) = g(\phi_o)$$

due to the 2π-periodicity of the vector field of (6).

(iii) $-2\pi < g(\phi_o) < +2\pi$, $\forall\phi_o$. We prove this by contradiction. Suppose $g(\phi_o) > 2\pi$ for some ϕ_o'. Then $\exists\,\phi_o''$ such that $g(\phi_o'') = 2\pi$ in view of the continuity of $g(\cdot)$ and that fact that $g(\phi_o)$ must have at least one zero. Hence,

$F(2q\pi,\phi_o'') = (2p\pi + \phi_o'') + 2\pi = \phi_o'' + 2(p+1)\pi \Rightarrow \mu = \frac{p+1}{q}$, which contradicts the assumption that $\mu = \frac{p}{q}$.

Thus, $g(\phi_o)$ is continuous, bounded and 2π-periodic, and because of the smoothness of the right-hand side of (6), it is a function of bounded variation, which means that it will have an even number of zeros on the interval $[0,2\pi]$. Consequently, there is an even number of periodic solutions. A limiting case of interest is when there are only two zeros which coincide to produce only one periodic solution.

9. Non-periodic Solutions on the Surface of a Torus

A consideration of irrational values of the turning point (μ) leads to the discussion of non-periodic oscillatory motions. Indeed, if the turning point is irrational, the trajectories certainly do not close upon themselves on the torus to produce a periodic oscillation of ϕ, nor do they approach an equilibrium point. Thus, a non-periodic oscillation is obtained. Further properties of this motion are developed in the following analysis.

The zero meridian of the torus is the circular locus of $T = 0$. We define a mapping M which associates the initial condition $\phi(0)$ (which lies on the

zero meridian) to the point at which the trajectory emanating from $\phi(0)$ next intersects the zero meridian, i.e., M: $\phi(0) \to F\left(2\pi, \phi(0)\right)$. This is an application of the shooting method [18] to the problem on the torus. The composition of the mapping with itself K times means that

M^k: $\phi(0) \to F\left(2K\pi, \phi(0)\right)$. From Theorem 5, if $\mu = p/q$ and $\phi(0)$ lies on a periodic trajectory, then

$$M^q\phi(0) = \phi(0) + 2p\pi$$
$$= \phi(0) \pmod{2\pi}$$

If $\phi_o = \phi(0)$, we define the nth successive point ϕ_n of ϕ_o as $\phi_n \triangleq M^n\phi_o \pmod{2\pi}$. ϕ_{n1} is said to follow ϕ_{n2} if, moving along the zero meridian starting from ϕ_o along the direction of increasing ϕ, we first encounter ϕ_{n1} and then ϕ_{n2}. We denote this by $\phi_o \alpha \phi_{n1} \alpha \phi_{n2}$. If $\langle a \rangle$ denotes the fractional part of the real number a, the following relationship is obtained between the successive points of ϕ_o.

Theorem 7: For any μ, rational or irrational

$$\langle \mu q_1 \rangle < \langle \mu q_2 \rangle \Rightarrow \phi_o \alpha \phi_{q_1} \alpha \phi_{q_2}$$

and

$$\langle \mu q_2 \rangle < \langle \mu q_1 \rangle \Rightarrow \phi_o \alpha \phi_{q_2} \alpha \phi_{q_1}$$

Proof: See [17].

If μ is irrational, we know from Theorem 5 that no trajectory on the torus $\Sigma' \times T'$ will close upon itself. Without loss of generality we can study the behavior of the trajectory with initial condition $\phi_o = 0$. Let $\mathcal{S}(\mu)$ be the set of successive points of ϕ_o, i.e., $\mathcal{S}(\mu) \triangleq \{\phi_k \mid k=1,2,\ldots\}$, and $\mathcal{P}(\mu)$ be the set of accumulation points of $\mathcal{S}(\mu)$.

Lemma: If μ is irrational, then $\mathcal{P}(\mu)$ is a perfect set (i.e., the set is closed and everywhere dense).

Proof: See [17].

Theorem 8: For solutions of (6) and irrational μ, the set $\mathcal{P}(\mu)$ covers the entire zero meridian of $\Sigma' \times T'$.

Proof: See

This result is very important for obtaining a convenient picture of how a

trajectory with an irrational turning point occupies the surface of a torus. The trajectory covers the entire zero meridian densely, and by extension covers the complete surface of the torus densely. A simple example of such a trajectory is $\phi(T) = \mu T$, where μ is irrational; clearly, if T is a multiple of 2π, then μT cannot be a multiple of 2π and as T progresses, the trajectory gradually covers the entire torus. It is not suprising that any trajectory with an irrational μ is topologically equivalent to the trajectory $\mu T + \phi_o$, as stated in the following corollary, which is proved, along with the next corollary in [17].

Corollary 1: If the turning point μ is irrational (and $\mathcal{P}(\mu)$ coincides with the entire zero meridian), then there exists a homeomorphism of the torus onto itself such that the trajectories of (6) are carried into the trajectories of $\frac{d\phi}{dT} = \mu$.

Another consequence of Theorem 8 is:

Corollary 2: The mapping M satisfies the ergodic hypothesis [19].

Under these conditions, an anlytic form can be given to these densely covering trajectories [20]:

Theorem 9: There exists a function ω: $\mathbb{R}^2 \to \mathbb{R}$ which is continuous and satisfies $\omega(x,y) = \omega(x+2\pi,y) = \omega(x,y+2\pi)$ such that every solution of (6) can be written as

$$\phi(T) = \mu T + c + \omega(T, \mu T + c) \text{ where } c \text{ is a constant.}$$

Conversely, for any constant c, $\phi(T)$ defined above solves (6), and to each value of c (modulo 2π) there corresponds a unique ϕ_o.

Proof: See Appendix 3. ¤

Corollary: The waveform $\mu T + c + \omega(T, \mu T + c)$ defines an almost periodic trajectory on the surface of the torus $\mathcal{T}' \times T'$.

An almost periodic waveform is not periodic, but is best defined by comparison with a periodic waveform. If x(t) has period T, then

$$|x(t + T) - x(t)| = 0$$

for all values of T. However, if x(t) is almost periodic, then if we choose an arbitrarily small $\varepsilon > 0$, there is a length $L(\varepsilon)$ such that

$$|x(t+T) - x(t)| < \varepsilon$$

for all t, and $T < L(\varepsilon)$, where T depends in general on the initial time t. A precise definition of almost periodicity, along with some of its more

interesting properties are given elsewhere [14]. Here, we simply state the following two properties which are of direct interest:

(i) If $\phi(u)$ is almost periodic, then so is $\frac{d\phi}{du}$.

(ii) The average value of $\phi(u)$ is well-defined and independent of u if $\phi(u)$ is almost periodic.

The averaging process used in (7) to interpret the turning point as the average normalized junction voltage is thus consistent for both rational and irrational values of μ.

10. Structural Stability of the Turning Point

If a given R.H.S. of (6) yields a turning point μ, is it possible to perturb the R.H.S. in some manner such that the turning point of the perturbed system also has value μ? We restrict ourselves to additive perturbation functions of the form $f_p(T,\phi)$, where $f_p(T,\phi) = f_p(T + 2\pi,\phi) = f_p(T, \phi + 2\pi)$, so that the essential features of the differential equation remain unchanged. The turning point of the unperturbed system is said to be structurally stable if there exists some $\varepsilon > 0$ so that any additive perturbation $f_p(T,\phi)$ with $|f_p(T,\phi)| < \varepsilon$ yields the same turning point for the perturbed differential equation.

The following result is central for structural stability:

Theorem 10: Equation (6) has a structurally stable turning point (μ) if, and only if, μ is rational and the determining function $g(\phi_o)$ changes sign on the interval $[0,2\pi)$.

Corollary: Because the right-hand side of (6) is analytic, its turning point μ is structurally stable if, and only f, it has at least one asymptotically stable periodic solution.

We have shown previously in Section 8 that $g(\phi_o)$ is a bounded, continuous and 2π-periodic function of bounded variation, so that a transversal intersection with the axis is sufficient to guarantee structural stability of the turning point, according to Theorem 10. The Corollary could be used to show the structural stability of a rational turning point if the method of Lyapunov were applied to ascertain the asymptotic stability of the periodic trajectory as suggested in [21]; readers who have some experience in finding Lyapunov

functions will know that this is not a simple task.

Finally, Theorem 10 establishes that all irrational turning points are structurally unstable.

An important physical consequence of these results is that only structurally stable solutions can be experimentally observed; structural instability means that the continually present perturbations due to noise, etc. in any experiment will change the character of the solutions.

From the circuit theoretic point of view the turning point can be interpreted as the normalized average junction voltage. For the instantaneous junction voltage is

$$v(t) = \frac{\bar{h}}{2e} \frac{d\phi}{dt}$$

whence the average junction voltage becomes

$$V_{dc} \triangleq \lim_{t\to\infty} \frac{1}{t} \int_0^t \frac{\bar{h}}{2e} \frac{d\phi(u)}{du}\, du = \frac{\bar{h}}{2e} \lim_{t\to\infty} \frac{\phi(t) - \phi(0)}{t}$$

$$= \frac{\bar{h}}{2e} \lim_{T\to\infty} \frac{\phi\left(\frac{T}{\omega}\right) - \phi(0)}{\left(\frac{T}{\omega}\right)} = \frac{\bar{h}}{2e} \lim_{T\to\infty} \frac{\phi\left(\frac{T}{\omega}\right)}{\left(\frac{T}{\omega}\right)}$$

$$= \frac{\omega\bar{h}}{2e} \lim_{T\to\infty} \frac{F(T,\phi_o)}{T} \quad \left(\text{where } \phi(0) = \phi_o\right)$$

$$= \frac{\omega\bar{h}}{2e} \times \mu \qquad \ldots(7) \tag{7}$$

$$\therefore \quad \mu = \frac{V_{dc}}{\frac{\omega\bar{h}}{2e}} \triangleq \frac{V_{dc}}{\hat{V}} \qquad \text{where } \hat{V} \triangleq \frac{\omega h}{2e} = I_o R \times \Omega \tag{8}$$

11. The I-V Characteristics of an a.c. Excited Josephson Junction

Typical I-V characteristics of a direct current applied to a junction in the presence of an a.c. excitation are shown in Fig. 7(b), and their singular feature is the appearance of constant voltage steps. We now explain the mechanism of these steps using the results on the stability of turning points developed in the preceding section.

Recall the differential equation (6) defining the junction dynamics

$$\frac{d\phi}{dT} = A_{dc} + A_o \sin\phi - A_{ac} \sin T$$

Corresponding to a given d.c. input A_{dc}, the solution trajectories of (6) define a unique turning point $\mu(A_{dc})$.

Thus, a unique point defined by the coordinates $(\mu(A_{dc}), A_{dc})$ is obtained in the normalized I-V plane, remembering that μ is merely the normalized average junction voltage. The results in the preceding Section indicate that the junction voltage waveform is periodic if the normalized voltage is rational, and almost periodic if it is irrational.

Consider the effect of increasing the d.c. input from A_{dc} to $A_{dc} + \delta A_{dc}$, where $\delta A_{dc} > 0$. Two observations are now in order.

Observation 1: The turning point, μ, varies continuously with changes in A_{dc}.

Proof: Choose an $\varepsilon > 0$. Let $\frac{p_1}{q_1} \in (\mu, \mu+\varepsilon)$, which means that $\frac{p_1}{q_1} \in$ Class 1 of $\mu(A_{dc})$ as defined in Section 8. By the analytic continuity of the solution of (6) with the parameter A_{dc} [14], there exists a $\rho > 0$ such that for all $A'_{dc} \in (A_{dc} - \rho, A_{dc} + \rho)$, the trajectory $F'(T, 0)$ generated by the differential equation

$$\frac{d\phi}{dT} = (A'_{dc} + A_o \sin \phi - A_{ac} \sin T)$$

will pass below the grid point $(2q\pi, 2p\pi)$ of the spaces $\sum$ x T; i.e., $\frac{p_1}{q_1} \in$ Class 1 for $\mu(A'_{dc})$. Therefore,

$$\text{given } \varepsilon > 0, \exists\, \beta > 0 \ni |A'_{dc} - A_{dc}| < \beta \Rightarrow |\mu(A'_{dc}) - \mu(A_{dc})| < \varepsilon \qquad \square$$

Observation 2: The turning point, μ, increases monotonically with A_{dc}.

Proof: Let the trajectory passing through the origin in $\sum$ x T due to excitation A_{dc} be $F(T,0)$, and the trajectory due to an increased excitation $A_{dc} + \delta A_{dc}$ ($\delta A_{dc} > 0$) be $F_\delta(T,0)$. Then $F_\delta(T,0) > F(T,0)$ for $T > 0$ because $\frac{d\phi}{dT}$ for the perturbed system is greater at each point of the space $\sum$ x T. Thus, some elements of Class 1 of the unperturbed system might become elements of Class 2 of the perturbed system, but no elements of Class 2 of the unperturbed system will become elements of Class 1 of the perturbed system; in short, the Dedekind cut of Fig. 10(b) might be a more positive number for the perturbed system.

$\therefore\ \mu(A_{dc} + \delta A_{dc}) \geq \mu(A_{dc})$. $\square$

Whenever there exists a $\delta A_{dc} > 0$ such that $\mu(A_{dc} + \delta A_{dc}) = \mu(A_{dc})$, the turning point due to A_{dc} is structurally stable. Theorem 10 assures us that this can only happen when $\mu(A_{dc})$ is a rational number. This means that a constant voltage

step exists at this voltage $\mu(A_{dc})$, when a change in current (δA_{dc}) does not produce a change in the voltage (μ). Constant voltage steps thus only occur when the average junction voltage is a rational multiple of $\frac{\overline{h}}{2e} \times \omega$, and this is indeed experimentally observed.

No equilibrium points $\left(\text{where } \frac{d\phi}{dt} = 0\right)$ can exist for the a.c. excited system due to the sinusoidal forcing term on the right-hand side. This means that unlike the d.c. excited system, the current observed in the characteristics of Fig. 7(b) is not a supercurrent, but is merely a large constant voltage step, much like those appearing at other voltages throughout the characteristics. The preceding dicussion shows that the instantaneous junction voltage here will be a periodic waveform whose average value must be exactly zero.

12. Evaluating the Heights of Constant Voltage Steps

The existence of the constant voltage steps is now established. The question which naturally arises next is: What determines the heights of these steps? In particular, when do steps whose height is zero occur? We have not found convenient analytical answers to these questions, but have obtained some insight into the mechanism of step production by the qualitative considerations which now follow.

The maximum upper bound on the heights of the steps is first obtained. If both sides of (6) are averaged with respect to time assuming $\mu(A_{dc}) = \frac{p}{q}$, we obtain

$$\mu = \frac{p}{q} = A_{dc} \quad \frac{A_o}{2q\pi} \quad \int_0 \sin\phi(T)\,dT$$

$$\text{Now}^5 \; -1 \leq \frac{1}{2q\pi} \int_0^{2q\pi} \sin\phi(T)\,dT \leq +1$$

which means that on a constant voltage step, we must have[6]

$$\Delta\,\mu(A_{dc}) = 0 = \Delta A_{dc} \pm A_o\,\Delta\left\{\frac{1}{2q\pi} \int_0^{2q\pi} \sin\phi(T)\,dT\right\} \leq \Delta A_{dc} \pm 2A_o$$

so that $|\Delta A_{dc}| \leq 2A_o$.

---

[5] If the function $\sin\phi(T)$ is periodic on the T axis, then its average value must lie between +1 and −1.

[6] In words, to maintain μ constant, any change in the average value of $\sin\phi(T)$ must be compensated by an equal and opposite change in A_{dc}.

The height of a constant voltage step thus must be less than $2A$. In particular, the step at $V_{dc} = 0$ cannot exceed the maximum supercurrent.

Recall the determining function defined as $g(\phi_o) \triangleq F(2q\pi,\phi_o) - (\phi_o+2p\pi)$ for a rational turning point $\mu = \frac{p}{q}$. A typical graph of $g(\phi_o)$ vs. ϕ_o satisfying the properties stated in Section 8 is shown in Fig. 11(a); each zero crossing of the graph corresponds to a distinct periodic solution.

Observation: Let ϕ_o^* be a zero-crossing point; i.e., $g(\phi_o^*) = 0$. The periodic solution at ϕ_o^* is locally asymptotically stable if, and only if, $\frac{dg}{d\phi}|\phi_o^* < 0$.

Proof: As the velocity field on $\sum' \times T$ is C^∞ function, $g(\phi_o)$ will be a C^∞ function. Thus, there is an ε-neighborhood of ϕ_o^* on which $\frac{dg}{d\phi_o} < 0$. Therefore, $\phi \in (\phi_o^*,\phi_o^*+\varepsilon)$ means $g(\phi_o) < 0$; i.e., $F(2q\pi,\phi_o) < \phi_o + 2p\pi \Leftrightarrow F(2q\pi,\phi_o) < \phi_o \pmod{2}$ so the non-periodic trajectory starting from ϕ_o tends to the periodic trajectory through ϕ_o^*. This argument is illustrated in Fig. 11(b). The sufficiency proof is obvious. ∎

Let us now turn to examining the step heights using the determining function. The structural stability of a rational turning point has a convenient interpretation in terms of the graph of the associated determining function: if this function intersects the ϕ_o-axis transversally at a point, it will continue to intersect it for a small enough perturbation if A_{dc} in the right-hand side of (6), so that periodic solutions satisfying $F(2q\pi,\phi_o) = \phi_o + 2p\pi$ will exist for both the original and the perturbed systems. This amounts to the structural stability of this turning point (μ), where the original and perturbed values of A_{dc} are two values of d.c. excitations on the constant voltage step at μ.

Given that $g(\phi_o)$ intersects the ϕ_o-axis transversally, the height of the corresponding step is determined by the values of positive and negative perturbations, respectively, that can be applied to A_{dc} so that $g(\phi_o)$ for the perturbed system intersects the ϕ_o-axis tangentially. This argument is graphically summarized in Fig. 12. We note that if A_{dc}^{max} and A_{dc}^{min} are the maximum and minimum values of A_{dc} on a step of constant voltage, then $g_{max} \triangleq \left\{g(\phi_o) \,|\, \phi_o \in [o,2\pi]\right\} = 0$ with A_{dc}^{max} on the R.H.S. of (6) and $g_{min} \triangleq \left\{g(\phi_o) \,|\, \phi_o \in [o,2\pi]\right\} = 0$ with A_{dc}^{min} on the R.H.S. of (6) (or vice-versa).

It would be possible to numerically calculate the height of the step at a given voltage if we knew one point (A_{dc},μ) on the step; if the corresponding determining function for μ (where μ must be a rational number) intersected the ϕ_o-axis transversally the turning point would be structurally stable and the

step then would have a non-zero height. This height can be found by perturbing A_{dc} both positively and negatively until the determining function intersects the ϕ_o-axis tangentially: the difference between these perturbations is then the step height. A numerical integration procedure is required to evaluate each values of the determining function.

The problem is how to obtain the initial point (A_{dc},μ). If we select A_{dc} and numerically solve (6) there is no means of deducing numerically whether the resulting turning point is rational. However, we can turn the problem around and fix μ to be a rational number by choosing integers p and q (such that $\mu = \frac{p}{q}$); then if we can find an A_{dc} such that $(A_{dc},\frac{p}{q})$ is an admissible pair on the I-V characteristics, defined by (6), we can proceed to apply perturbations to A_{dc}. Suppose the a.c. excitation in (6) is set to zero

$$\text{i.e.} \quad \frac{d\phi}{dT} = A_{dc} + A_o \sin\phi \qquad \ldots \quad (9)$$

This differential equation can be solved analytically [22] to obtain

$$T = \frac{2}{\sqrt{(A_{dc})^2 - (A_o)^2}} \arctan\left\{\sqrt{\frac{A_{dc}-A_o}{A_{dc}+A_o}} \quad \frac{1 + \tan(\phi/2)}{1 - \tan(\phi/2)}\right\}$$

$$\text{whence} \quad \mu = \lim_{T\to\infty} \frac{\phi(T)}{T} = \sqrt{A_{dc}^2 - A_o^2} \qquad \ldots \quad (10)$$

Fixing μ by choosing $\frac{p}{q}$ we can determine A_{dc} from (10). This is the value of A_{dc} that would be obtained on the characteristics in the absence of a.c. excitation. If a small a.c. excitation is now applied so that

$$\frac{d\phi}{dT} = A_{dc} - A_o \sin\phi + \varepsilon \sin T$$

where $\varepsilon > 0$ is small, the resulting value of A_{dc} to maintain $\mu = p/q$ will shift by a small amount. This observation suggests the following algorithm:

Given: p, q, and a numerical integration subroutine.

Step 1: Set $x = A_{dc}$ obtained from (10) with $\mu = \frac{p}{q}$.

Step 2: Define $g(\phi_o) = F(2q\pi,\phi_o) - (2p\pi+\phi_o)$ obtained from integrating (6) with $A_{dc} = x$.

Check whether $g(\phi_o)$ has zeros on the interval $[1,2\pi]$: if yes, go to Step 4.

Step 3: Set $x = x+\delta$, where $\delta > 0$ is some suitably small number.

Return to Step 2.

Step 4: (x,μ) is an admissible signal pair on the I-V characteristics. Now apply perturbations to x to determine the heights of the steps. ¤

This algorithm can provide the heights of constant voltage steps at least for a small a.c. excitation of amplitude ε, and should numerically confirm the observed step heights for $\mu = o, \frac{1}{1}, \frac{2}{1}, \frac{3}{1}, \ldots, \frac{1}{2}, \frac{1}{3}, \ldots, \frac{2}{3}, \frac{2}{5}, \ldots$, etc.

13. A Phase Locking Interpretation of the Characteristics of an a.c. Excited Josephson Junction

Anderson [23] originally suggested the appearance of constant voltage steps in the a.c. excited characteristics as the result of a process of synchronization and many papers since [24, 25] have developed models of the junction which display step-like behavior in their characteristics due to this phenomenon. The results of our analysis provide, for what we believe is the first time, a precise understanding of this phenomenon.

A constant voltage step can appear in the I-V characteristics, as the preceding analysis shows, only when the turning point has a rational value $\frac{p}{q}$; i.e., the frequency of oscillation of the instantaneous junction voltage (ω_j) $= \frac{p}{q}$ x the frequency of the a.c. excitation (ω_{in}), as explained in Section 7. Furthermore, ω_j can be considered as an oscillation frequency controlled by the d.c. excitation, as suggested in the last paragraph of Section 4. Thus, a constant voltage step occurs whenever the continuously variable ω_j is a rational multiple of the applied ω; in particular, when the qth harmonic of ω_j synchronizes with the pth harmonic of ω.

The height of the step is an indication of the entrainment range of this synchronization; roughly speaking, variations in A_{dc} over the height of the step would tend to change ω_j, but the synchronization process causes ω_j to be entrained by ω_{in} and maintain the turning point at a constant value. It is precisely this reason why the phase-locked loop model of Bak [10] successfully simulates the I-V characteristics of the a.c. excited junction. This circuit is shown in Fig. 13, and provides a very convenient experimental means of displaying our arguments. The locking ranges for the harmonic/subharmonic synchronization taking place in the phase-locked loop circuit then correspond to the step heights.

14. Extension of Results to General Synchronization Phenomena

A more general statement of the phenomenon of synchronization is as follows: there exists an autonomous system $\dot{\underset{\sim}{x}} = \underset{\sim}{f}(\underset{\sim}{x})$ with a stable limit cycle of period T, to which is applied an oscillatory excitation force of period T', with the result that the period of oscillation of the autonomous system is entrained to T' by the excitation.

Suppose the autonomous system has a state space Σ on which its dynamics are determined by a time-invariant direction field. The effect of the applied excitation is to impose a T'-periodic perturbation on the direction field, and synchronization occurs if this time-varying direction field has a new limit cycle in Σ with period T'.

This time-varying direction field in Σ is equivalent to a T'-periodic velocity field uniquely defined at each point of the space Σ x t, where t is the time variable. The limit cycle of the autonomous system generates an integral manifold which is a cylinder in Σ x t, i.e., if $L(\underset{\sim}{x}) \subset \Sigma$ is the limit cycle, where $L(\underset{\sim}{x}) \triangleq \left\{ \underset{\sim}{x}(t) \,\middle|\, t\in[o,T),\ \underset{\sim}{x}(t+T) = \underset{\sim}{x}(t) \right\}$, then this cylinder is $L(\underset{\sim}{x})$ x $[o,\infty)$. If a suitably small excitation is applied so that $\dot{\underset{\sim}{x}} = \underset{\sim}{f}(\underset{\sim}{x}) + \varepsilon\, \underset{\sim}{g}(t)$ (where $\underset{\sim}{g}(t+T') = \underset{\sim}{g}(t)$) and synchronization is obtained, then we should expect a closed curve in Σ denoted by $L_\varepsilon(\underset{\sim}{x})$ such that $L_o(\underset{\sim}{x}) = L(\underset{\sim}{x})$ and $\underset{\sim}{x}(T', \underset{\sim}{x}_o) = \underset{\sim}{x}_o$ for any $\underset{\sim}{x}_o \in L_\varepsilon(\underset{\sim}{x})$. This idea is illustrated in Fig. 14 and was originally suggested by Levinson [26]. An integral manifold which has the shape of a distorted "cyclinder" is generated by all the trajectories with initial conditions on $L_\varepsilon(\underset{\sim}{x})$. Because the endpoints of the "cylinder" at t=o and t=T' are identical and the velocity field defined on the surface of this "cylinder" is also identical at these points, the two ends of the "cylinder" can be joined together smoothly to form a "torus." The advantage of doing so is that all the preceding theory of flows on a torus, which is presented in a general form as flows on 2-manifolds in [13] can then be applied to this problem, and the conditions for the existence and stability of closed trajectories on the "torus" obtained. These closed trajectories are precisely the synchronized solutions.

A recent Russian text [27] contains the latest results for the dynamics on such a "torus".

15. Conclusions

The features of the d.c. I-V characteristics of a Josephson junction have been explained in terms of the flows on a cylindrical phase space. The junction

phase difference (ϕ) attains an equilibrium point in the supercurrent regime, and acts like a current-controlled oscillator in the finite voltage regime. The hysteresis in these characteristics is due to the co-existence of an equilibrium point and a periodic solution.

For the a.c. excited Josephson junction, the dynamics are described for a simpler circuit model as trajectories on the surface of a torus. Using the concept of a turning point to define the various possibilities of periodic flows on the torus, the character of harmonic and subharmonic oscillatory waveforms is defined. Furthermore, the existence of almost periodic waveforms is established. The presence of constant voltage steps is related to the strucutral stability of the turning point, which roughly means that the character of a periodic oscillation is not affected by small enough perturbations in the excitation. An algorithm is suggested to numerically determine the heights of these constant voltage steps.

A precise interpretation is finally provided for how an a.c. excited junction is subject to synchronization phenomena, and that the step height is merely the entrainment range, or locking range, of each synchronization event. It is then shown how synchronization, in general, can be geometrically interpreted as closed trajectories on an integral manifold which can be smoothly transformed into an n-dimensional "torus."

REFERENCES

[1] Josephson, B. D., "Possible new effects in superconductive tunnelling," Physics Letters, vol. 1, p. 251, 1962.

[2] Thomsen, D. E., "Measuring Minute Magnetics," Science News, vol. 111, no. 15, p. 234, April 9, 1977.

[3] "Josephson junction logic and memory circuits," Physics Today, June 1978.

[4] Waldram, J. R., A. B. Pippard and J. Clarke, "Theory of the current-voltage characteristics of SNS junctions and other superconducting weak links," Phil. Trans. of Roy. Soc. of London, vol. 268A, p. 265, Nov. 1970.

[5] Stewart, W. C., "Current-voltage characteristics of Josephson junction," Applied Physics Letters, vol. 12, no. 8, p. 277, April 15, 1968.

[6] McCumber, D. E., "Effect of a.c. impedance on d.c. voltage-current characteristics of superconductor weak-link junctions," Journal of Applied Physics, vol. 39, no. 7, p. 3113, June 1968.

[7] Sullivan, D. B., R. L. Peterson, V. E. Kose and J. E. Zimmerman, "Generation of Harmonics and subharmonics of the Josephson oscillation," Journal of Applied Physics, vol. 41, no. 12, p. 4865, November 1970.

[8] McCumber, D. E., "Tunneling and weak link superconductor phenomena having potential device applications," Journal of Applied Physics, vol. 39, p. 2503, 1968.

[9] Hansma, P. K. and G. I. Rochlin, "Shunted junction and mechanical model results," Journal of Applied Physics, vol. 43, no. 11, November 1972.

[10] Bak, C. K. and N. F. Pedersen, "Josephson junction analog and quasiparticle-pair current," Applied Physics Letters, vol. 22, no. 4, p. 149, February 15, 1973.

[11] Shapiro, S., "Josephson currents in superconducting tunneling: The effect of microwaves and other observations," Physical Review Letters, vol. 11, no. 2, p. 80, July 15, 1963.

[12] Chua, L. O., Introduction to Nonlinear Network Theory, McGraw-Hill, New York, 1969.

[13] Hartman, P., Ordinary Differential Equations, John Wiley and Sons, New York, 1964.

[14] Hale, J. K., Ordinary Differential Equations, Wiley-Interscience, New York, 1969.

[15] Langenberg, D. N., D. J. Scalapino and B. N. Taylor, "Josephson-type superconducting tunnel junctions as generators of microwave and submillimeter wave radiation," Proc. IEEE, vol. 54, no. 4, p. 560, April 1966.

[16] Poincaré, H., Les methodes nouvelles de la mechanique celeste, Gauthier-Villers, Paris, 1892, 1893 and 1899 (3 vols.).

[17] Pliss, V. A., Nonlocal Problems of the Theory of Oscillations, Academic Press, New York, 1966.

[18] Aprille, T. J., Jr., and T. N. Trick, "Steady state analysis of nonlinear circuits with periodic inputs," Proc. IEEE, vol. 60, pp. 108-114, Jan. 1972.

[19] Halmos, P. R., Lectures on Ergodic Theory, Math. Soc. Japan, Tokyo, 1956.

[20] Coddington, E. A. and N. Levinson, Theory of Ordinary Differential Equations, McGraw-Hill, New York, 1955.

[21] Yoshizawa, T., Stability Theory of Lyapunov's Second Method, Math. Soc. Japan, Tokyo, 1966.

[22] Greenhill, Sir A. G., Differential and Integral Calculus, Macmillan, New York, 1396.

[23] Anderson, P. W., "Considerations on the flow of superfluid helium," Reviews of Modern Physics, vol. 38, no. 2, p. 298, April 1966.

[24] Anderson, P. W., "The Josephson effect and quantum coherence measurements in superconductors and superfluids," in Progress in Low Temperature Physics, vol. 5, 1967.

[25] Fack, H. and V. Kose, "Pull-in phenomena of Josephson oscillations," Journal of Applied Physics, vol. 42, no. 1, p. 320, January 1971.

[26] Levinson, N., "Small periodic perturbations of an autonomous system with a stable orbit," Annals of Mathematics, vol. 52, no. 3, p. 727, November 1950.

[27] Boguliobov, N. N., J. A. Mitropoliskii and A. M. Samoilenko, Methods of Accelerated Convergence in Nonlinear Mechanics, Springer, New York, 1976.

Appendix 1

Theorem 1. If a unique solution $y = \phi(x)$ of (4) through (x_o, y_o) exists for all $x > x_o$ in $\sum$, and is bounded, then it is either 2π x-periodic or asymptotically approaches some 2π x-periodic solution as $x \to \infty$.

Proof. If $\phi(2\pi) = \phi(0)$, then due to the time-invariance of the R.H.S. of (4), the solution is 2π x-periodic. This is the trivial case.

Suppose, without loss of generality, that $\phi(2\pi) > \phi(0)$. Then the sequence $\{\phi(2k\pi)\}$, $K = 1,2,\ldots$, tends to a limit as $k \to \infty$. The sequence is clearly bounded by hypothesis. Suppose that it is not monotonic i.e. suppose $\phi(4\pi) \leq \phi(2\pi)$. Let $y = \psi(x)$ be the solution of (4) with initial condition $\psi(2\pi) = \phi(0)$. By the periodicity of the direction field of (4),

$$\psi(x) \equiv \phi(x-2\pi), \quad \forall x.$$

$$\Rightarrow \psi(4\pi) = \phi(2\pi) > \phi(4\pi) \text{ as assumed above.}$$

But $\psi(2\pi) = \phi(0) < \phi(2\pi)$ by construction.

$\therefore \exists\ \tilde{x} \in (2\pi, 4\pi)$ s.t. $\phi(\tilde{x}) = \psi(\tilde{x})$. But this contradicts uniqueness, so $\phi(4\pi) > \phi(2\pi)$.

By induction, $\phi(2(K+1)\pi) > \phi(2K\pi)$, all integers K. $\Rightarrow$ the sequences is monotonic. By the axiom of completeness, a bounded monotone sequence has a limit (a,say).

Next, we observe that the solution $y = \chi(x)$ of (4) with $\chi(0) = a$ is 2π x-periodic. For if $\phi_K(x) \triangleq \phi(x+2\pi K)$, K integer, then $\phi_K(x)$ is a solution of (4) due to the 2π x-periodicity of the direction field. Moreover, from what we have shown above, $\lim \phi_K(0) = a$. By continuity, $\phi_K(2\pi) \to \chi(2\pi)$ as $K \to \infty$. But $\phi_K(2\pi) = \phi((K+1)2\pi) \overset{K\to\infty}{\to} a$ as $K \to \infty$. $\Rightarrow \chi(2\pi) = a = \chi(0)$. $\Rightarrow$ $y = \chi(x)$ is 2π x-periodic.

Finally, notice that $\phi(x)$ asymptotically approaches (x) as $x \to \infty$. For any solution of (4) depends continuously on its initial condition, so that given $\varepsilon > 0, \exists\ \delta > 0$ s.t. for $y = y(x)$, $|y(0) - \ | < \delta \Rightarrow |y(x)-\chi(x)| < \varepsilon$, $\forall x \in [0,2\pi]$. As $\{\phi(2\pi K)\} \to a$, choose K_1 large enough so that $|\phi(2\pi K)-a| < \varepsilon$ for $\forall K \geq K_1$.

$$|\phi(x) - \chi(x)| < \varepsilon \text{ for } \forall x \geq 2\pi K_1.$$

Thus, $\phi(x)$ asymptotically tends to $\chi(x)$.

The theorem is thus established. ∎

Appendix 2

Accurate plots of the solution flows of (4) in Σ corresponding to various values of α and β_c are shown in Fig. A-1. The direction field is represented by the field of small arrows, the corresponding flows by thin solid lines and the separate trajectory by thick solid lines. The equilibrium points are represented by the pairs of thick dots on the x-axis. In Fig. A-1 (d), (e) and (f), the thick dotted lines are 2π x-periodic flows.

We now interpret these phase plane portraits in terms of the d.c. I-V characteristics of the junction (Fig. 2). Note that in Fig. A-1 (a), (b) and (c) all flows, irrespective of initial condition, tend to a stable equilibrium point where $y \equiv \dot{\phi} = 0$. This corresponds to the supercurrent regime in the I-V characteristics where a finite current ($\alpha>0$) can be sustained at zero voltage ($\dot{\phi}=0$). In Fig. A-1(d) a flow will either tend to a stable equilibrium point or to a 2π x-periodic flow depending on the initial condition. The 2π x-periodic flow will yield a periodic waveform for $\phi(t)$, so that a non-zero average value of ϕ will exist. Thus, in this case, a supercurrent or a finite voltage state can both be obtained, and this corresponds to the hysteresis in the I-V characteristics. Finally, in Fig. A-1(e) and (f), all the flows tend towards a 2π x-periodic flow, and this is the finite-voltage regime in the I-V characteristics.

Quantitative considerations of the hysteresis in the I-V characteristics

McCumber [6] has calculated the minimum value of α required to enter the hysteresis loop in the I-V characteristics of the d.c. excited junction: this corresponds to I_c in Fig. 2. He has thus obtained a plot of this critical value (α_c) vs. the normalized junction capacitance (β_c), by what he implies to be numerical solutions of the differential equation (DC).

Based on the insight we have obtained from the phase plane portraits, we can formulate a simple means to obtain a similar plot. In terms of these portraits, for a given β_c, α_c is the smallest value of α which will yield a 2π x-periodic trajectory. If we are only interested in determining the existence of periodic trajectories, the "shooting method" of numerical analysis can be used by defining the following function for (4):

$$F(\phi_o) \triangleq \tilde{y}(2\pi;\phi_o)$$

where $\tilde{y}(x;\phi_o)$ is the solution of the implicit differential equation (4) with initial condition ϕ_o using a numerical integration procedure. Then any fixed point of the map $F: \phi_o \to \tilde{y}(2\pi;\phi_o)$ approximates a point on a 2π x-periodic solution within the accuracy of the numerical procedure.

Using the forward Euler method of integration and plotting $F(\phi_o)$ vs. ϕ_o for various values of β_c for each α we obtained the plots of Fig. A-3. The intersection of $F(\phi_o)$ with the st. line of unit slope through the origin thus determined the fixed points of the map F. Notice that there exists a minimum value of $\phi_o = \phi_o^{min}$ below which the $F(\phi_o)$ curve does not exist; this minimum is determined by the initial condition separatrix trajectory on the phase plane portraits, for the flows in $\sum$ with initial condition $< \phi_o^{min}$ do not exist throughout the interval $[0,2\pi]$.

Given α, the values of β_c were varied until intersection with the straight line was just obtained: the value of α gave α_c for this critical β_c. The plot of our computer predicted α_c vs. β_c agreed very well with that of McCumber's in Fig. A-2.

Appendix 3

Theorem 3: Let q and p be factorized as $q = Kq_1$ and $p = Kp_1$ (where K is an integer > 1), and assume that the grid point $(2q\pi,2p\pi)$ lies above (resp., below, on) the trajectory F(T,0). Then the point $(2q_1\pi,2p_1\pi)$ will also lie above (resp., below, on) the trajectory.

Proof: If the trajectory F(T,0) lies below the grid point $(2q\pi,2p\pi)$ then it lies below $(4q\pi,4p\pi)$ and in general below $(2nq\pi,2np\pi)$. We see this by considering the solution trajectory $\phi(T)$ of (6) which passes through the point $(2q\pi,2p\pi)$. By uniqueness, $\phi_1(T) > F(T,0)$, $\forall$ T.

$$\therefore \quad \phi_1(4q\pi) > F(4q\pi,0). \tag{3.1}$$

Now note the following property of these two trajectories: F(T,0) passes through the origin and $\phi_1(T)$ passes through the point $(2q\pi,2p\pi)$. As (6) defines a 2π-periodic velocity field, $F(T,0) = \phi_1(T+2q\pi) - 2p\pi$. Thus,

$$F(2q\pi,0) = \phi_1(4q\pi) - 2p\pi = \phi_1(4q\pi) < 4p\pi \tag{3.2}$$

From (3.1) and (3.2), $F(4q\pi,0) < 4p\pi$ i.e., the trajectory F(T,0) passes below the grid point $(4q\pi,4p\pi)$. The argument can be repeated for any $(2nq\pi,2np\pi)$.

Assume now the contrary to the hypothesis of the theorem i.e., that $(2q\pi, 2p\pi)$ lies above the trajectory F(T,0) but $(2q_1\pi,2p_1\pi)$ does not. Then one of the following must hold:

(i) $(2q_1\pi,2p_1\pi)$ lies below the trajectory. But by the preceding arguments, this means that $(2Kq_1\pi,2Kp_1\pi)$ lies below the trajectory. This leads to a contradiction.

(ii) $(2q_1\pi,2p\pi)$ lies on the trajectory. But then by the 2π-periodicity of the velocity field, $(2Kq_1\pi,2Kp_1\pi)$ also lies on the trajectory, which again leads to a contradiction. Thus the theorem is proved. ∎

Theorem 4. Let μ be the turning point generated by a given right-hand side of (6). Then if $F(T,\phi_o)$ is the trajectory in $\sum \times T$ generated by (6) for any $\phi_o \in [0,2\pi)$, the following limiting relation holds:

$$\lim_{T\to\infty} \frac{F(T,\phi_0)}{T} = \mu$$

Proof: We establish the result by considering two special cases.

Special Case 1: $\lim_{n\to\infty} \frac{F(2n\pi,0)}{2n\pi} = \mu.$

Choose an $\varepsilon > 0$, a positive integer N s.t. $\varepsilon > \frac{2}{N}$ and an integer m s.t.

$$\frac{m-1}{N} < \mu < \frac{m+1}{N} \tag{3.3}$$

From the Dedekind cut intepretation of turning point, this inequality implies that the trajectory $F(T,0)$ passes below the grid point $(2N\pi, 2(m+1)\pi)$ and above the grid point $(2N\pi, 2(m-1)\pi)$. Thus,

$$2(m-1)\pi < F(2N\pi,0) < 2(m+1)\pi \tag{3.4}$$

Dividing (3.4) by $2N\pi$, and subtracting from (3.3)

$$-\frac{2}{N} < \mu - \frac{F(2N\pi,0)}{2N\pi} < \frac{2}{N}$$

$$\Rightarrow \quad \left|\mu - \frac{F(2N\pi,0)}{2N\pi}\right| < \varepsilon$$

As ε is made arbitrarily small, N must increase in inverse proportion so that

$$\lim_{N\to\infty} \left|\mu - \frac{F(2N\pi,0)}{2N\pi}\right| = 0.$$

Special Case 2: $\lim_{T\to\infty} \frac{F(T,0)}{T} = \mu.$

An arbitrary T can be written as $T = 2\pi n + T'$ where n is a sufficiently large integer so that $T' \in [0,2\pi)$. If (6) is expressed as an integral equation with zero initial condition, we get

$$\phi(T) \triangleq f(T,0) = F(2n\pi,0) + \int_{2n\pi}^{T} (A_{dc} - A_0 \sin\phi + A_{ac} \sin T)\, dT$$

$$\text{Now } \phi' \triangleq \int_{2n\pi}^{T} (A_{dc} - A_0 \sin\phi + A_{ac} \sin T)\, dT \leq \int_{2n\pi}^{T} (A_{dc} + A_0 + A_{ac})\, dT \leq (A_{dc} + A_0 + A_{ac})2\pi$$

Thus ϕ' is a bounded quantity.

$$\frac{F(T,0)}{T} = \frac{F(2n\pi,0)+\phi'}{2n\pi+T'} = \frac{\frac{F(2n\pi,0)}{2n\pi} + \frac{\phi'}{2n\pi}}{1 + \frac{T'}{2n\pi}}$$

Now as $T \to \infty$, $n \to \infty$ but ϕ' and T' remain bounded quantities.

$$\lim_{T\to\infty} \frac{F(T,0)}{T} = \lim_{n\to\infty} \frac{F(2n\pi,0)}{2n\pi} = \mu \quad \text{from Special Case 1.}$$

General Case: By uniqueness of the solutions of (6), its trajectories in $\sum \times T$ do not intersect, which yields the following inequality:

$$F(T,0) \leq F(T,\phi_0) \leq F(T,2k\pi) = F(T,0) + 2k\pi$$

$$\Rightarrow \quad \lim_{T\to\infty} \frac{F(T,0)}{T} \leq \lim_{T\to\infty} \frac{F(T,\phi_0)}{T} \leq \lim_{T\to\infty} \frac{F(T,0)}{T}$$

$$\Rightarrow \quad \lim_{T\to\infty} \frac{F(T,\phi_0)}{T} = \mu. \qquad \square$$

Theorem 5. There exists a periodic solution trajectory of (6) on the torus $\sum' \times T'$ which completes p rotations and q revolutions prior to closing upon itself if, and only if, the turning point $\mu = \frac{p}{q}$.

Proof: Sufficiency: If for some $\phi_0 \in (0,2\pi)$, $F(2q\pi,\phi_0) = \phi_0 + 2p\pi$, then by the 2π-periodicity of the velocity field, we have

$$\frac{F(2qn\pi,\phi_0)}{2qn\pi} = \frac{\phi_0}{2qn\pi} + \frac{p}{q}$$

$$\Rightarrow \quad \lim_{n\to\infty} \frac{F(2qn\pi,\phi_0)}{2qn\pi} = \mu = \frac{p}{q}$$

where the last interpretation of μ follows from Special Case 1 in the proof of Theorem 4.

Necessity. Define the function $g(\phi_0) = F(2q\pi,\phi_0) - (2p\pi+\phi_0)$. Then the zeros of $g(\phi_0)$ lie on closed solution curves on the torus $\sum' \times T'$. As $F(2q\pi,\phi_0)$ depends analytically on the initial condition ϕ_0, $g(\phi_0)$ is a continuous function of ϕ_0. Furthermore, $g(\phi_0) = g(\phi_0+2n\pi)$, $\forall n$ positive integers.

For the sake of contradiction, assume that (6) has no solution trajectories, which after executing p rotations and q revolutions, close upon themselves on the torus, i.e., $g(\phi_0) \neq 0$, $\forall\phi_0$. As $g(\phi_0)$ is continuous, it must always maintain a constant sign. For definiteness, assume that $g(\phi_0) > 0$, and let $\alpha \triangleq \inf g(\phi_0)$. Since g is both continuous and periodic, $\alpha > 0$ (strictly).

$$g(\phi_0) \geq \alpha > 0$$

$$\Rightarrow \quad F(2q\pi,\phi_0) \geq \phi_0 + 2p\pi + \alpha \qquad (3.5)$$

Let $\phi_1 \triangleq F(2q\pi,\phi_0)$. As (3.5) holds for all ϕ_0,

$$F(2q\pi,\phi_1) \geq \phi_1 + 2p\pi + \alpha \tag{3.6}$$

By the periodocity of the R.H.S. of (6), $F(2q\pi,\phi_1) \equiv F(4q\pi,\phi_0)$, whence (3.6) becomes

$$F(4q\pi,\phi_0) \geq F(2q\pi,\phi_0) + 2p\pi + \alpha$$

and using (3.5)

$$F(4q\pi,\phi_0) \geq \phi_0 + 4p\pi + 2\alpha$$

In fact, we can show using induction that

$$F(2nq\pi,\phi_0) \geq \phi_0 + 2np\pi + n\alpha, \text{ all integers } n \tag{3.7}$$

For suppose the inequality is satisfied for some n = m.
Then $F(2q\pi,\phi_m) \geq \phi_m + 2p\pi + \alpha$ where we have invoked (3.5) and $\phi_m \triangleq F(2mq\pi,\phi_0)$.
But $F(2q\pi,\phi_m) \equiv F(2q(m+1)\pi,\phi_0)$.

$$F(2q(m+1)\pi,\phi_0) \geq F(2qm\pi,\phi_0) + 2p\pi + \alpha$$

Combining this with (3.7) with n = m, we get

$$F(2q(m+1)\pi,\phi_0) \geq \phi_0 + 2(m+1)p\pi + (m+1)\alpha.$$

Thus, the inductive proof is complete.

Now, dividing (3.7) by $2nq\pi$

$$\frac{F(2nq\pi,\phi_0)}{2nq\pi} \geq \frac{p}{q} + \frac{\alpha}{2q\pi} + \frac{\phi_0}{2nq\pi}$$

and proceeding to the limit as n $\to \infty$

$$\mu \geq \frac{p}{q} + \frac{\alpha}{2q\pi} > \frac{p}{q}$$

which contradicts the hypothesis that $\mu = \frac{p}{q}$, and establishes necessity. □

Theorem 9. There exists a function $\omega: \mathbb{R}^2 \to \mathbb{R}$ which is continuous and satisfies $\omega(x,y) = \omega(x+2\pi,y) = \omega(x,y+2\pi)$ such that every solution of (6) can be written as

$$\phi(T) = \mu T + c + \omega(T,\mu T+c)$$

where c is a constant. Conversely, for any constant c, $\phi(T)$ defined above solves (6), and to each value of c (modulo 2π) there corresponds a unique ϕ_0.

Proof: Let the homeomorphism of Corollary 1 to Theorem 8 which carries the torus onto itself be h.

If $F(T,\phi_0)$ is the solution of (6), then by the periodicity of the field on the torus

$$F(T,\phi_0+2\pi) = F(T,\phi_0) + 2\pi \tag{3.8a}$$

$$F(T+2\pi,\phi_0) = F(T,M\phi_0) \tag{3.8b}$$

where the map M is defined in Section 9 of the text. Let $c \triangleq h(\phi_0) \Rightarrow \phi_0 = G(c) \triangleq h^{-1}(c)$. From the properties of h given in [20], the following is true for G:

$$G(c+2\pi) = G(c) + 2\pi \tag{3.9a}$$

$$MG(c) = G(c+2\pi\mu) \tag{3.9b}$$

Let $\tilde{F}(T,c) \triangleq F(T,G(c))$. Then by (3.8a) and (3.9a)

$$\tilde{F}(T,c+2\ ) = \tilde{F}(T,c) + 2\pi \tag{3.10}$$

By (3.8b) and (3.9b)

$$\tilde{F}(T+2\pi,c) = F(T+2\pi,G(c)) = F(T,MG(c)) = F(T,G(c+2\pi\mu)) = \tilde{F}(T,c+2\pi\mu) \tag{3.11}$$

Now define $\omega(T,z) \triangleq F(T,z-T) - z$, $\forall t,z \in \mathbb{R}$.
Then by (3.10) and (3.11):

$$\omega(T+2\pi,z) = \omega(T,z+2\pi) = \omega(T,z)$$

Setting $z \triangleq \mu u + c$,

$$\tilde{F}(T,c) = \mu T + c + \omega(T,\mu T+c)$$

which proves the thoerem.

The converse follows from the definitions of ω and c. ∎

FIGURE CAPTIONS

Fig. 1. The device model.

Fig. 2. Typical I-V characteristics with d.c. excitation.

Fig. 3. McCumber's calculation of the hysteresis in Fig. 2. (A plot of the variation of the critical current I_c with junction capacitance, using normalized values).

Fig. 4. (a) A typical trajectory in $\Sigma \times \tau$.
(b) The projection of the trajectory in Σ.

Fig. 5. Illustrating the transformation of the semi-infinite strip Σ into the surface of the cylinder Σ'.

Fig. 6. A perspective view of a trajectory in $\Sigma' \times \tau$.

Fig. 7. Circuit diagram of the a.c. excited junction.

Fig. 8. Illustrating the transformation of the square $\Sigma \times T$ into the surface of the torus. $\Sigma' \times T'$.

Fig. 9. The three types of closed trajectories which can exist on the torus.

Fig. 10. (a) Grid points in $\Sigma \times T$, and an example of a periodic trajectory starting with zero initial condition.
(b) Illustrating the Dedekind cut on the real line.

Fig. 11. (a) A typical graph of the determining function.
(b) Stable and unstable periodic solutions.

Fig. 12. Interpreting the step heights in terms of the variation in the determining function.

Fig. 13. A Phase Locked Loop model for the a.c. excited Josephson junction.

Fig. 14. Comparing the integral manifolds for the autonomous and the synchronized limit cycles.

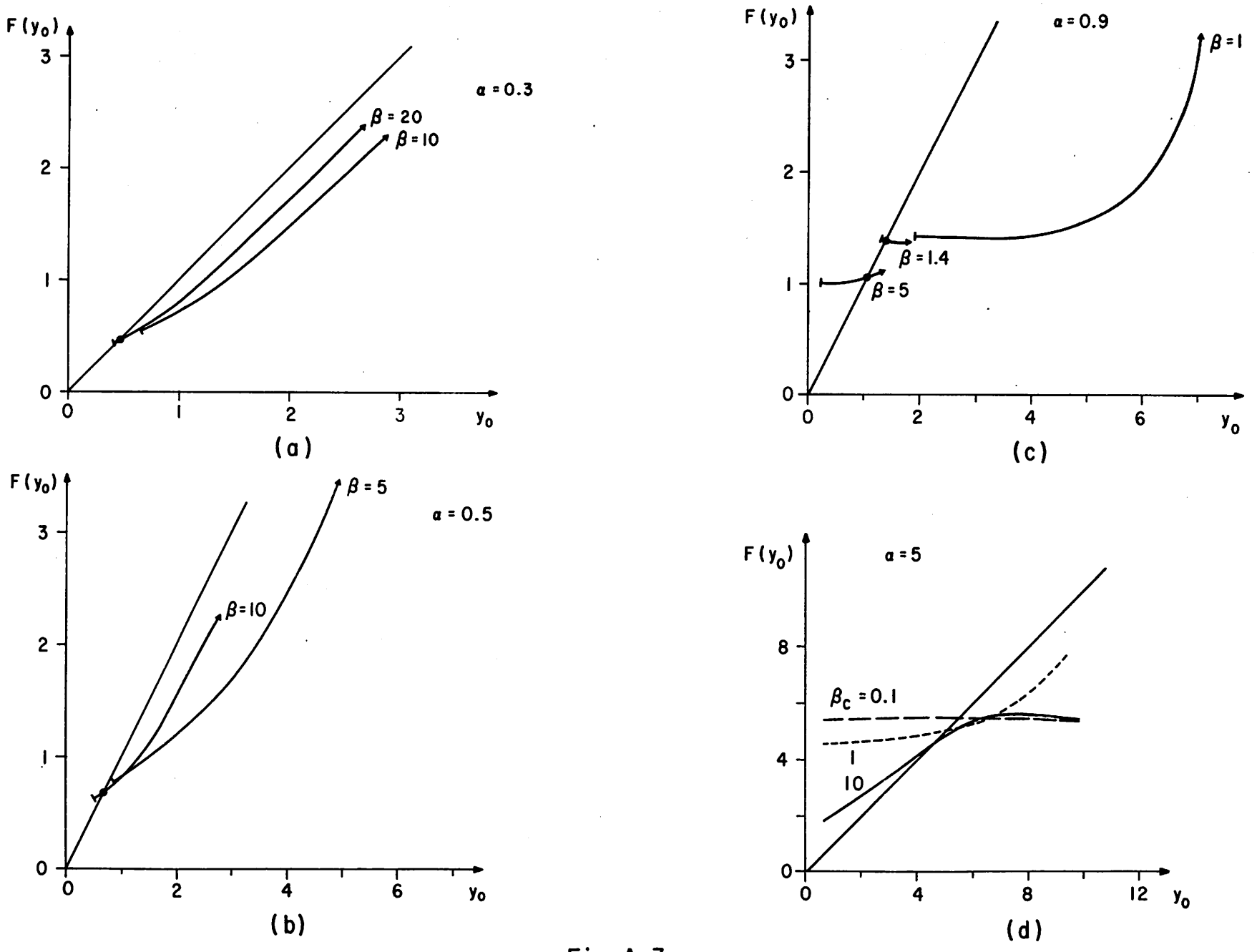
F(y0)
α = 0.3
β = 20
β = 10
y0
(a)
F(y0)
α = 0.5
β = 5
β = 10
y0
(b)
F(y0)
α = 0.9
β = 1
β = 1.4
β = 5
y0
(c)
F(y0)
α = 5
βc = 0.1
1
10
y0
(d)

Fig. A-3

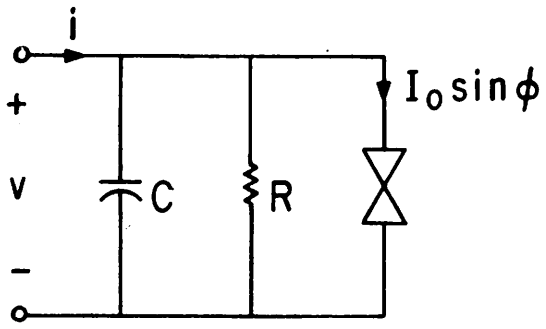

Fig. 1

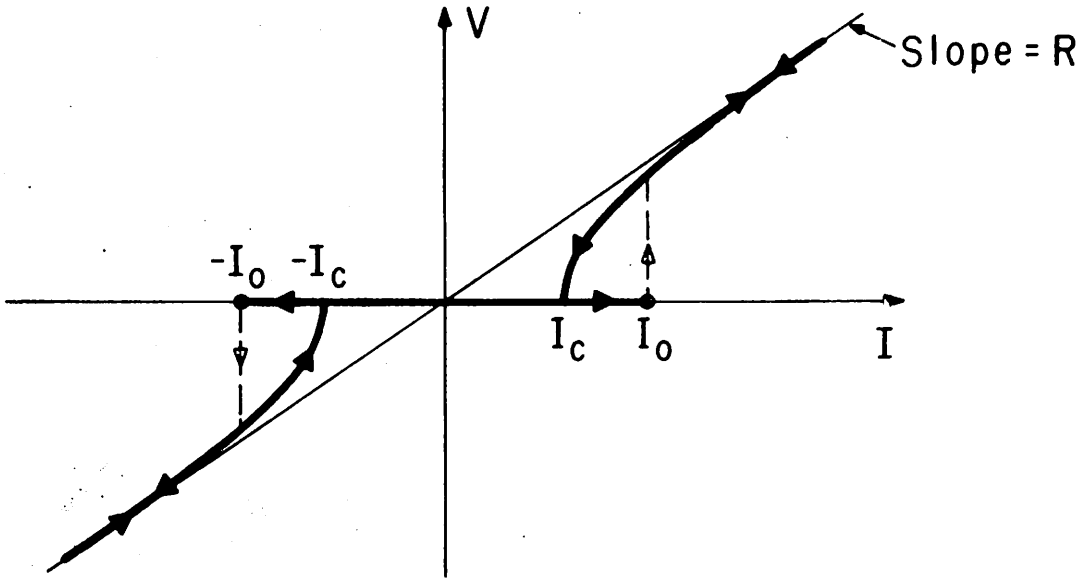

Fig. 2

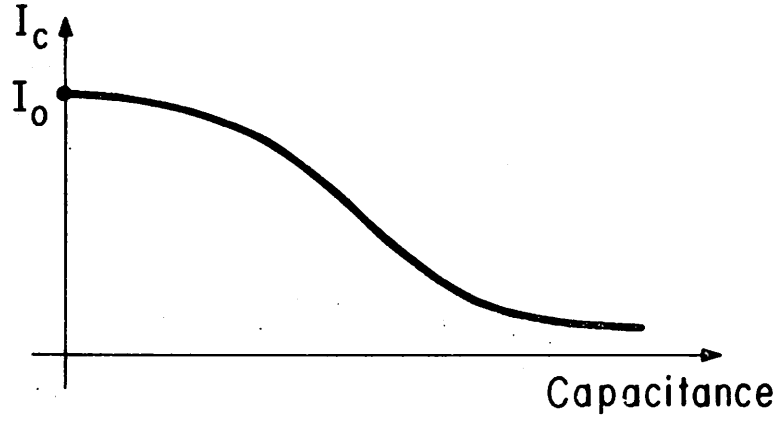

Fig. 3

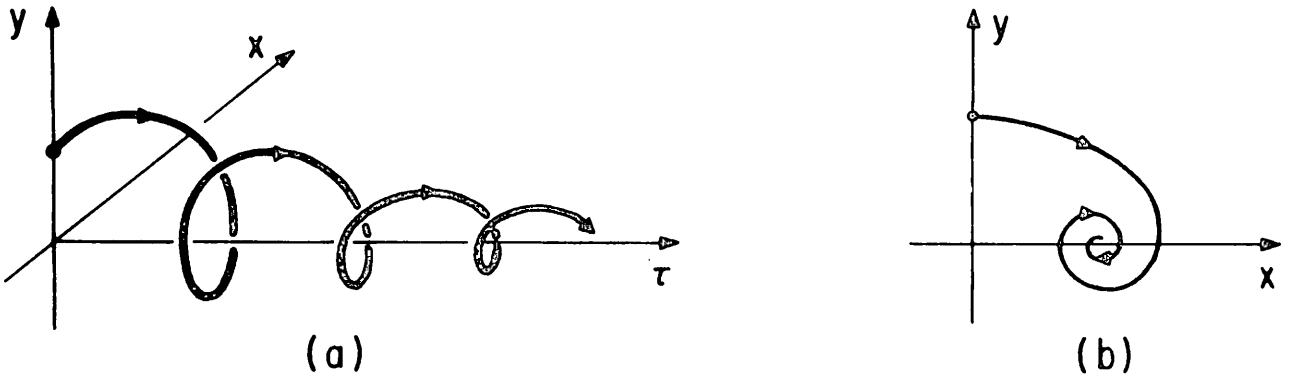

Fig. 4

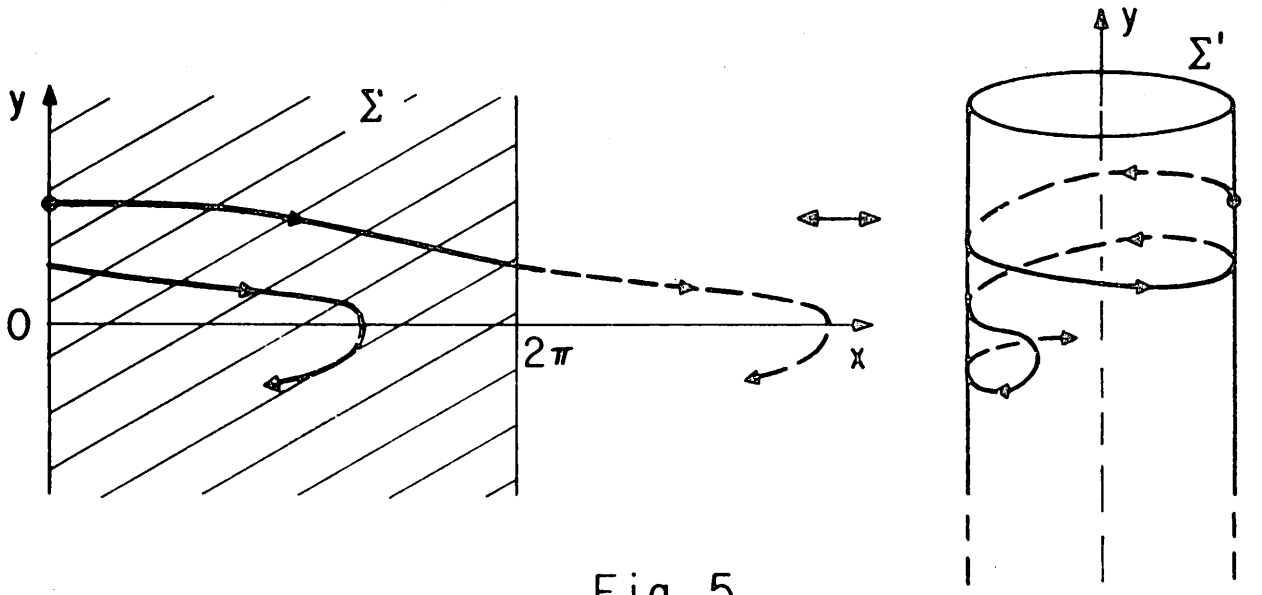

Fig. 5

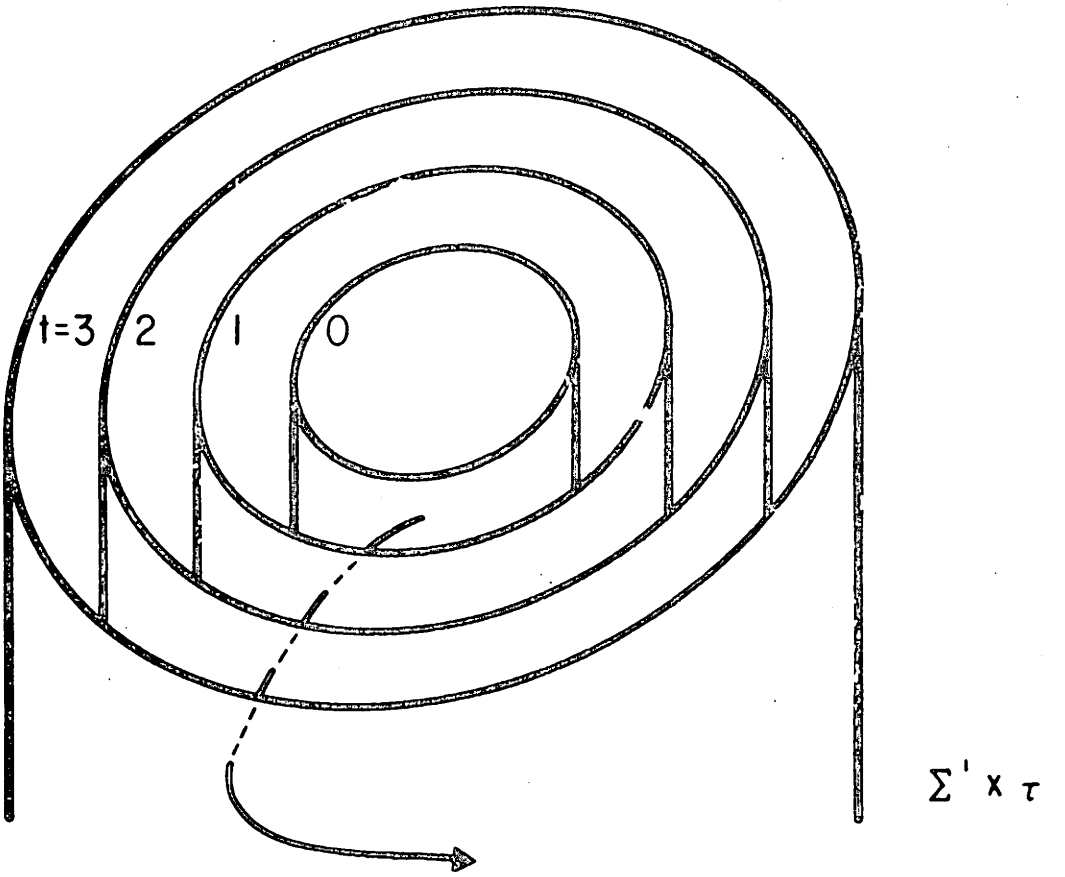

Fig. 6

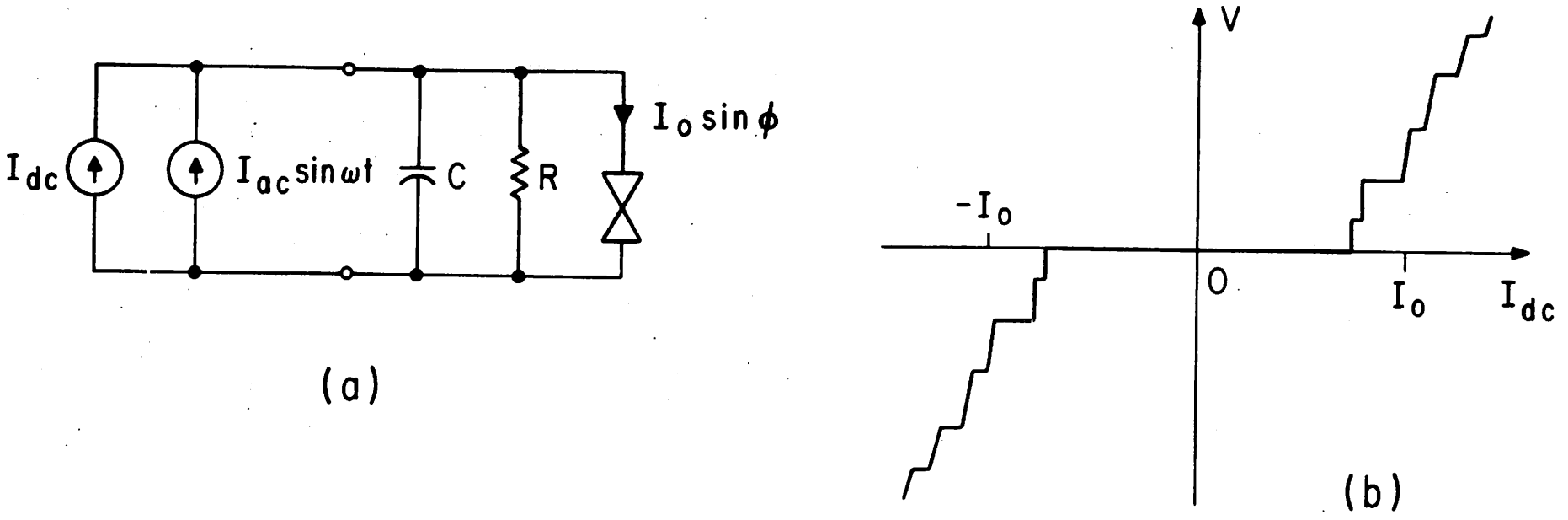
I_{dc}
$I_{ac}\sin\omega t$
C
R
$I_o \sin\phi$
(a)
V
$-I_o$
0
I_o
I_{dc}
(b)

Fig. 7

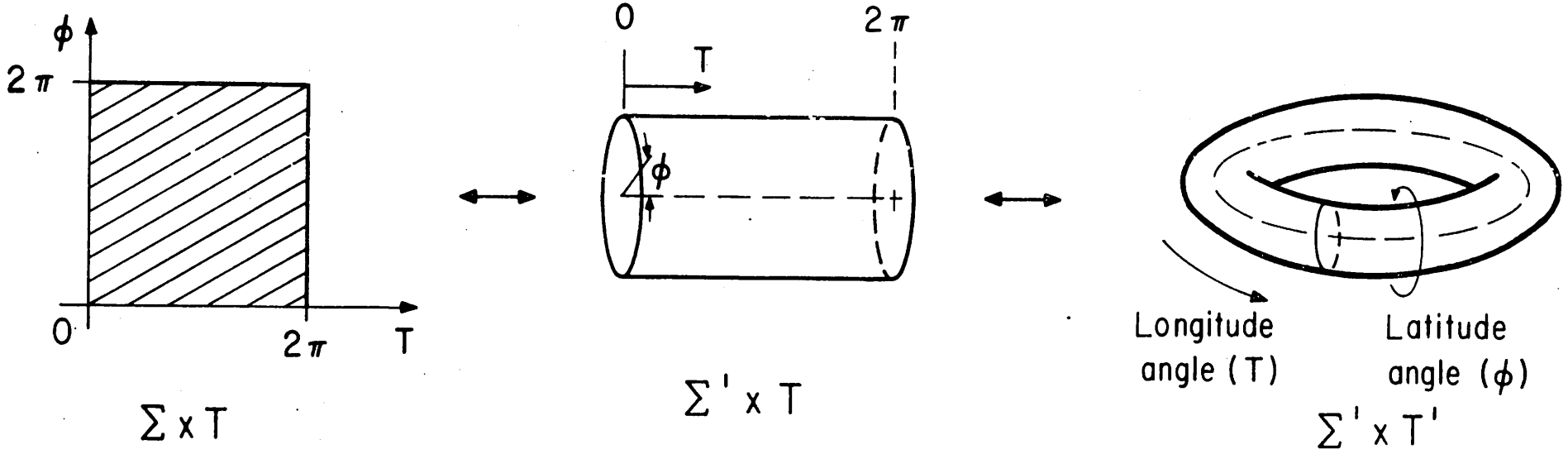
ϕ
2π
0
2π
T
$\Sigma \times T$
0
2π
T
ϕ
$\Sigma' \times T$
Longitude angle (T)
Latitude angle (ϕ)
$\Sigma' \times T'$

Fig. 8

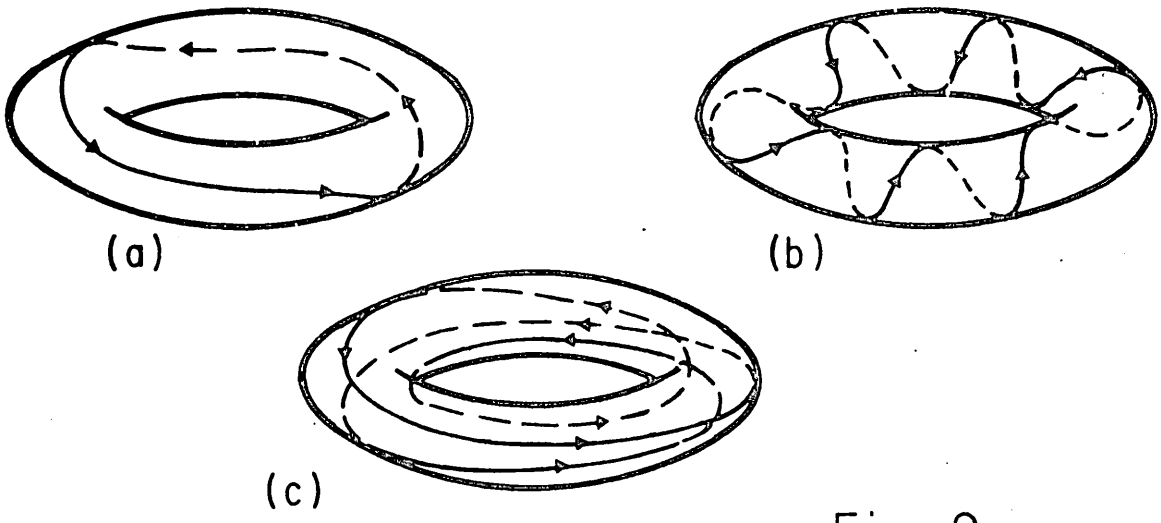

Fig. 9

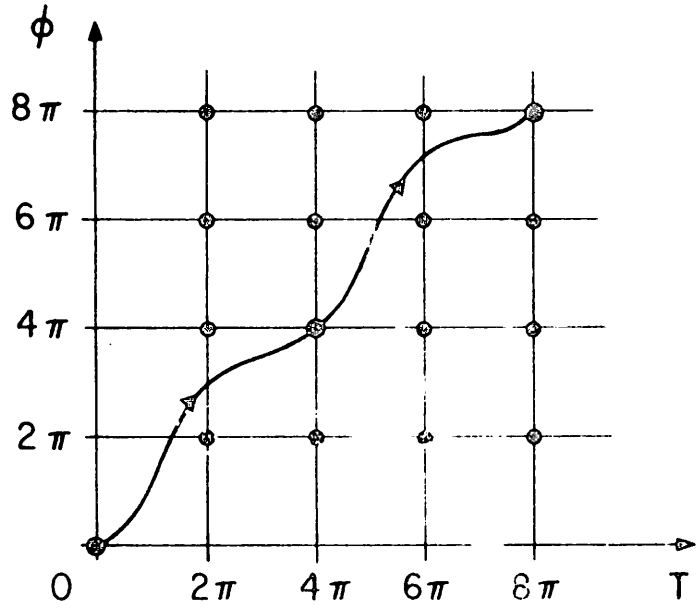

(a)

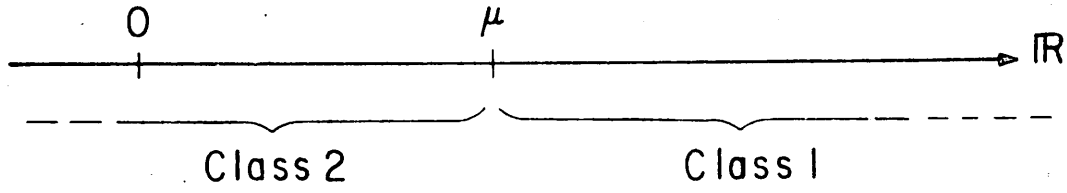

(b)

Fig. 10

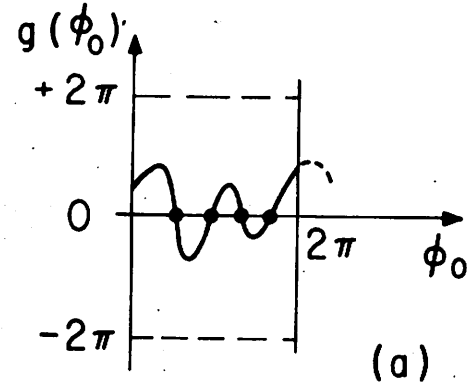

(a)

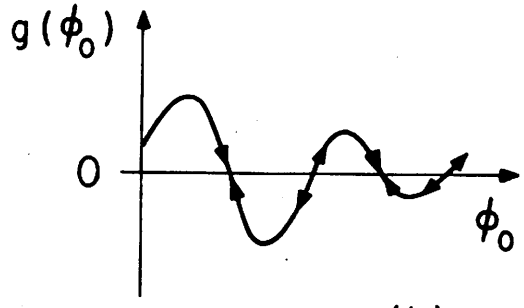

(b)

Fig. 11

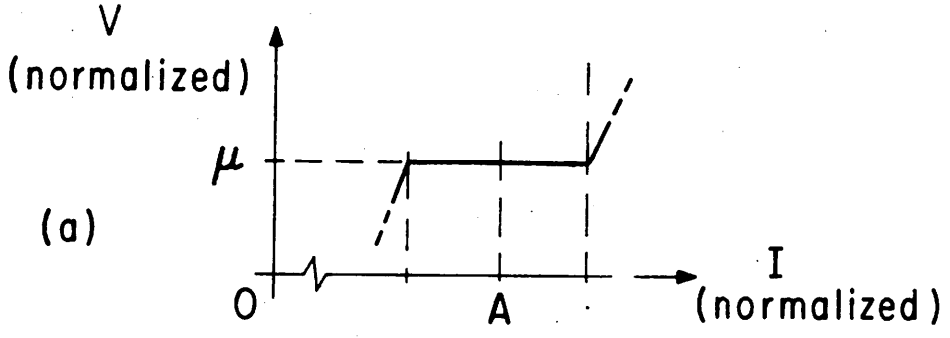

(a)

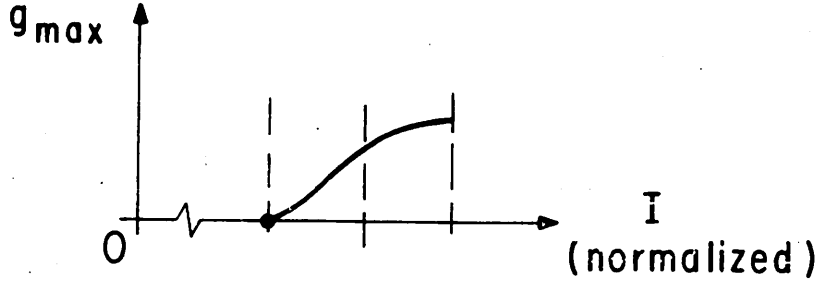

(b)

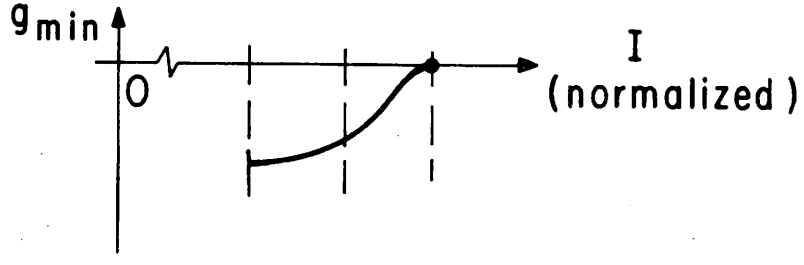

(c)

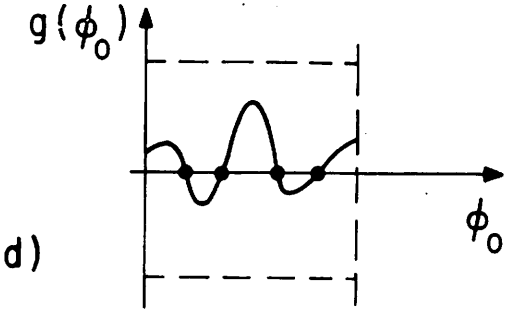

(d) Excitation = A

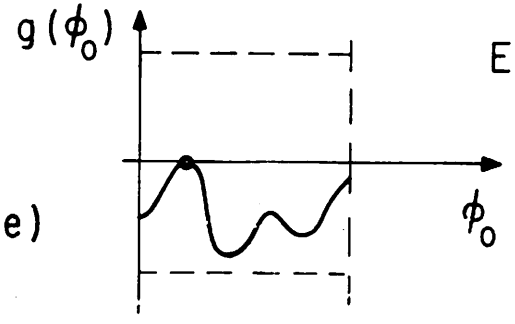

(e) Excitation = $A-\varepsilon_1$ $(\varepsilon_1>0)$

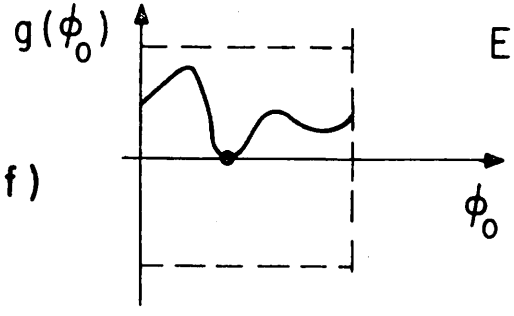

(f) Excitation = $A+\varepsilon_2$ $(\varepsilon_2>0)$

Fig. 12

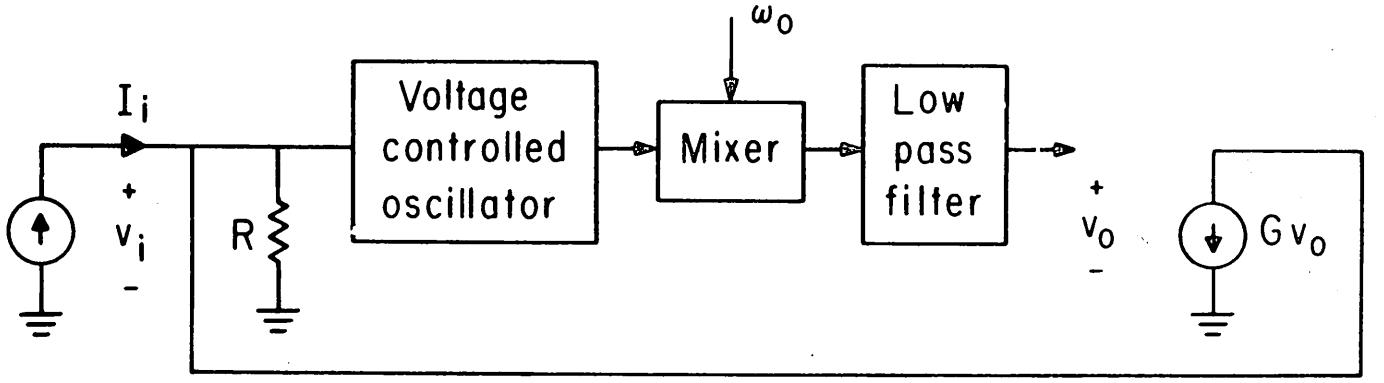
ω_0
I_i
+
v_i
-
R
Voltage controlled oscillator
Mixer
Low pass filter
+
v_0
-
Gv_0

Fig. 13

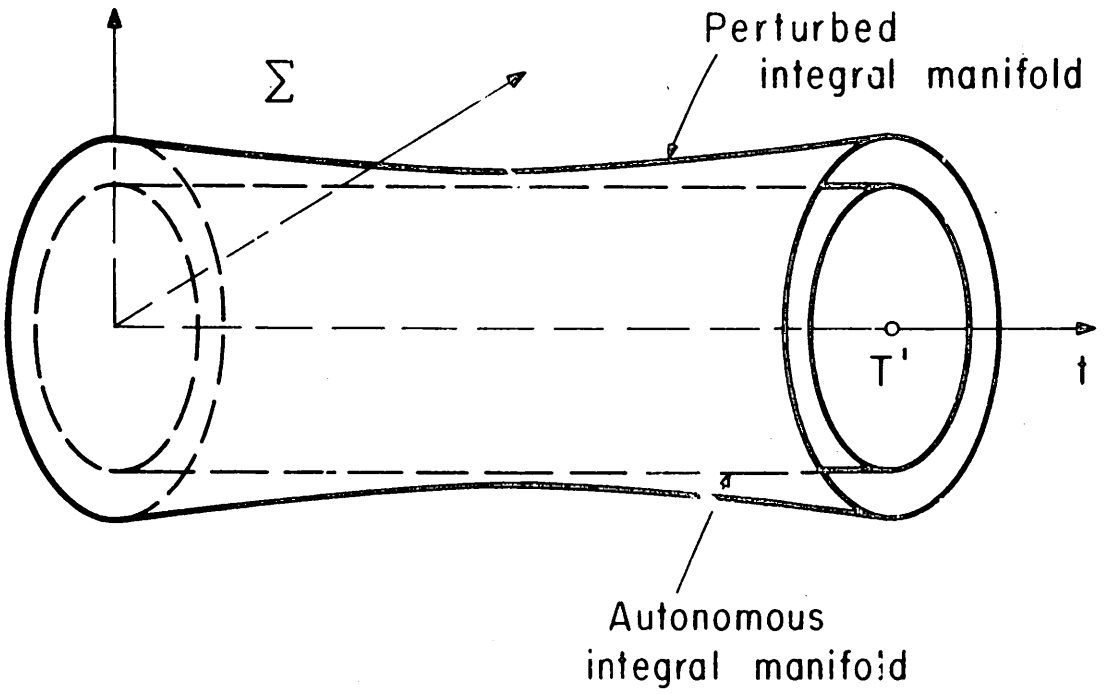
Σ
Perturbed integral manifold
T'
t
Autonomous integral manifold

Fig. 14

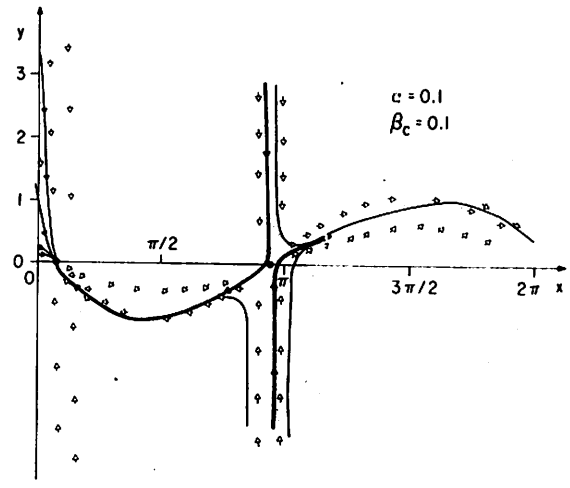

(a)

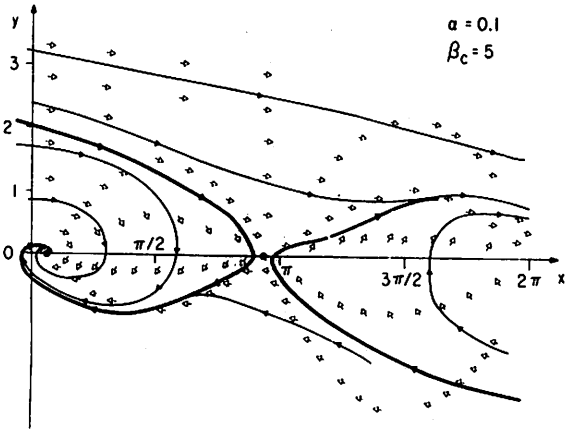

(b)

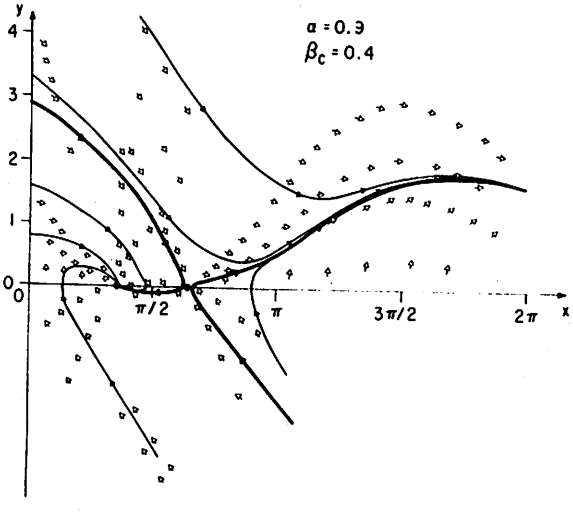

(c)

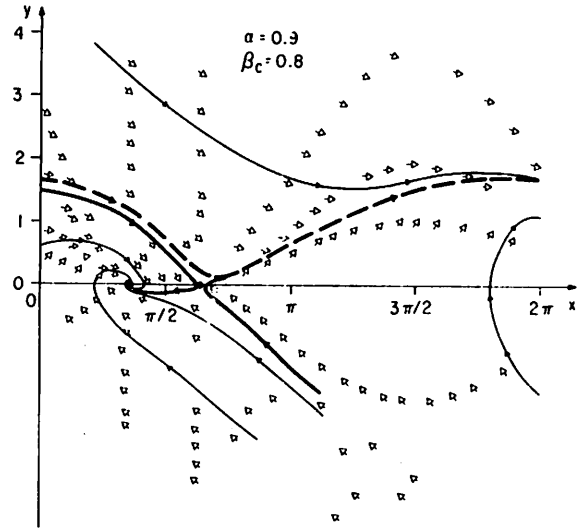

(d)

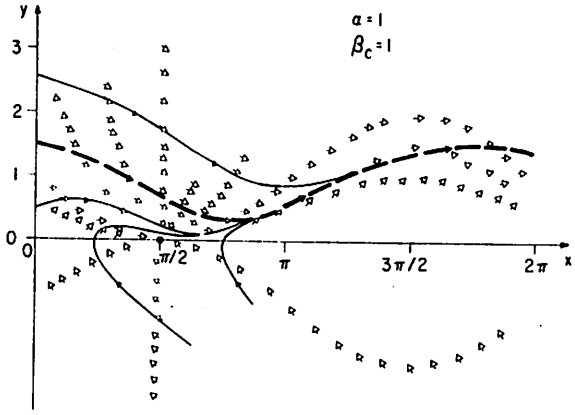

(e)

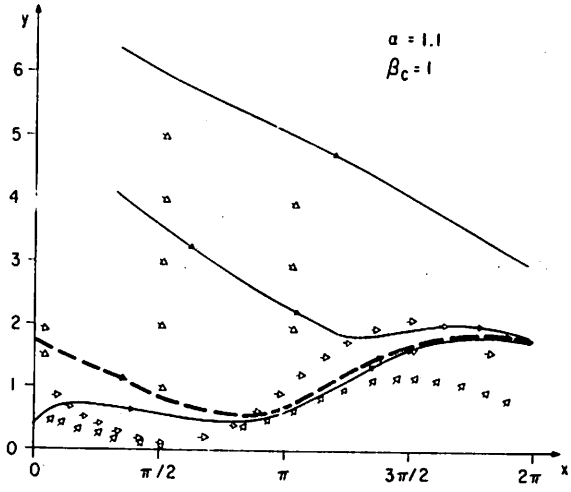

(f)

Fig. A-1

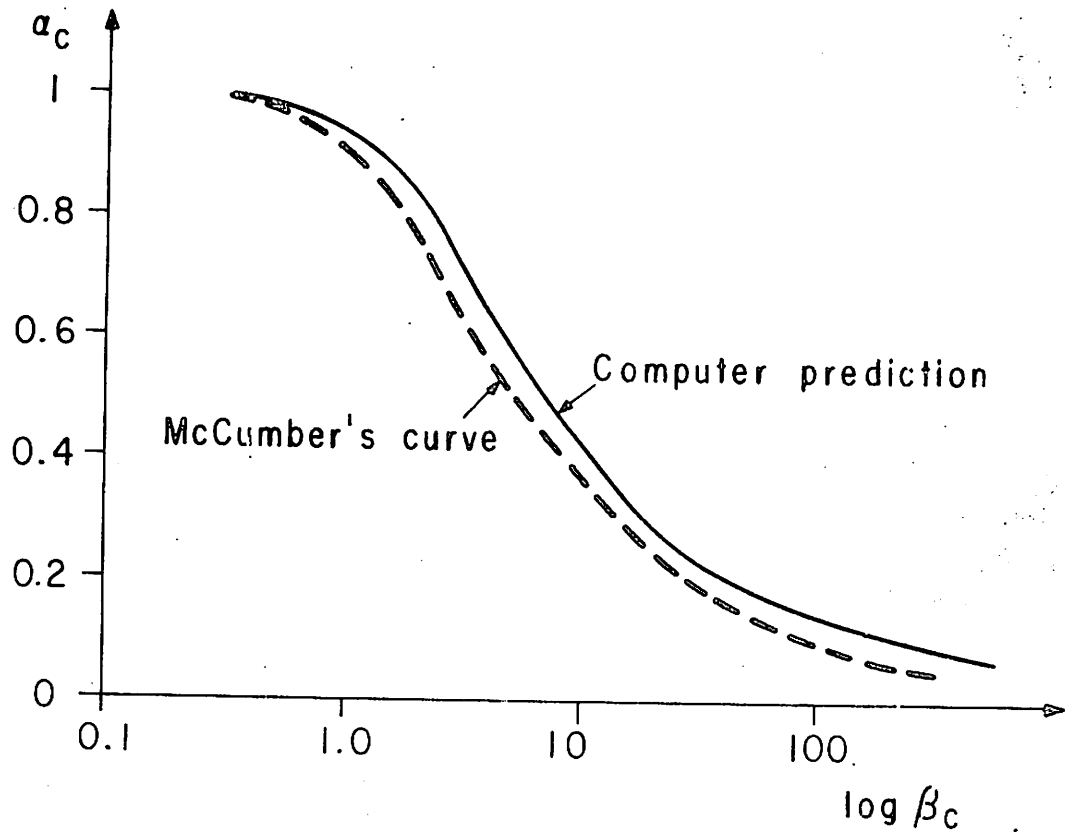
α_c
1
0.8
0.6
0.4
0.2
0
0.1
1.0
10
100
log β_c
Computer prediction
McCumber's curve

Fig. A-2